Visual Neuroscience (1993), **10**, 827-855. Printed in the USA.

Cortical afferents of visual area MT in the *Cebus* monkey: Possible homologies between New and Old World monkeys

MARCELLO G.P. ROSA,[1,2] JULIANA G.M. SOARES,[1]
MARIO FIORANI, JR.,[1] AND RICARDO GATTASS[1]

[1]Departamento de Neurobiologia, Instituto de Biofísica Carlos Chagas Filho, CCS, Bloco G, Ilha do Fundão, Rio de Janeiro 21941, Brazil
[2]Vision, Touch, and Hearing Research Centre, Department of Physiology and Pharmacology, University of Queensland QLD 4072, Australia

(RECEIVED October 19, 1992; ACCEPTED February 1, 1993)

Abstract

Cortical projections to the middle temporal (MT) visual area were studied by injecting the retrogradely transported fluorescent tracer Fast Blue into MT in adult New World monkeys (*Cebus apella*). Injection sites were selected based on electrophysiological recordings, and covered eccentricities from 2-70 deg, in both the upper and lower visual fields. The position and laminar distribution of labeled cell bodies were correlated with myeloarchitectonic boundaries and displayed in flat reconstructions of the neocortex. Topographically organized projections were found to arise mainly from the primary, second, third, and fourth visual areas (V1, V2, V3, and V4). Coarsely topographic patterns were observed in transitional V4 (V4t), in the parieto-occipital and parieto-occipital medial areas (PO and POm), and in the temporal ventral posterior area (TVP). In addition, widespread or nontopographic label was found in visual areas of the superior temporal sulcus (medial superior temporal, MST, and fundus of superior temporal, FST), annectent gyrus (dorsointermediate area, DI; and dorsomedial area, DM), intraparietal sulcus (lateral intraparietal, LIP; posterior intraparietal, PIP; and ventral intraparietal, VIP), and in the frontal eye field (FEF). Label in PO, POm, and PIP was found only after injections in the representation of the peripheral visual field (>10 deg), and label in V4 and FST was more extensive after injections in the central representation. The projections from V1 and V2 originated predominantly from neurons in supragranular layers, whereas those from V3, V4t, DM, DI, POm, and FEF consisted of intermixed patches with either supragranular or infragranular predominance. All of the other projections were predominantly infragranular. Invasion of area MST by the injection site led to the labeling of further pathways, including substantial projections from the dorsal prelunate area (DP) and from an ensemble of areas located along the medial wall of the hemisphere. In addition, weaker projections were observed from the parieto-occipital dorsal area (POd), area 7a, area prostriata, the posterior bank of the arcuate sulcus, and areas in the anterior part of the lateral sulcus. Despite the different nomenclatures and areal boundaries recognized by different models of simian cortical organization, the pattern of projections to area MT is remarkably similar among primates. Our results provide evidence for the existence of many homologous areas in the extrastriate visual cortex of New and Old World monkeys.

Keywords: Platyrrhyni, Visual cortex, Connections, Myeloarchitecture, Evolution

Introduction

Since its description by Allman and Kaas (1971), the middle temporal visual area (MT) has been one of the most intensively studied subdivisions of the extrastriate cortex. The middle temporal, primary (V1), and second (V2) visual areas are the only cortical visual areas for which a homology can be established with certainty across a wide range of primate species using a variety of independent criteria (*Aotus*: Allman & Kaas, 1971; *Galago*: Allman et al., 1973; *Macaca*: Gattass & Gross, 1981; Van Essen et al., 1981; *Cebus*: Fiorani et al., 1989; *Callithrix*: Spatz & Tigges, 1972; *Saimiri*: Tigges et al., 1981; *Miopithecus*: Kaas & Krubitzer, 1991). Area MT can be identified in all of the above-mentioned species by its heavy myelination, by the direct projections it receives from V1, and by its first-order represen-

Reprint requests to: Marcello G.P. Rosa, Vision, Touch, and Hearing Research Centre, University of Queensland, QLD 4072, Australia.

tation of the visual hemifield (Allman & Kaas, 1971; Lund et al., 1975; Spatz, 1977; Lin et al., 1982; Wall et al., 1982; Desimone & Ungerleider, 1986; Ungerleider & Desimone, 1986*a*,*b*; Fiorani et al., 1989; Krubitzer & Kaas, 1990; Sousa et al., 1991; Pessoa et al., 1992). MT also contains a large proportion of neurons sensitive to the direction of movement (Zeki, 1974; Van Essen et al., 1981; Maunsell & Van Essen, 1983*a*; Felleman & Kaas, 1984).

The boundaries and characteristics of other extrastriate visual areas are still the subject of considerable debate. There are conflicting models of the organization of simian extrastriate cortex, not only across studies of diverse genera, but also between studies of single genera like *Macaca* or *Aotus* (Fig. 1). These differences may result from a number of factors, including the phylogenetic history of the animals, interspecific allometric effects (Fleagle, 1988), possible effects of ecological niche on the development of the visual system and, last but not least, the different methods and criteria used by different investigators. The involvement of the last factor is, in part, supported by the conflicting models generated to describe the extrastriate organization of a single genus (e.g. Fig. 1). Conversely, when similar methods are used, the same general subdivisions of extrastriate cortex can be defined in primate species that are widely separated in evolutionary terms, as are representatives of Strepsirhini, Platyrrhini, and Catarrhini (Kaas & Krubitzer, 1991; Preuss & Goldman-Rakic, 1991). However, there is experimental evidence to support each of the different models, and it is difficult at present to choose the one closest to a generalized primate plan, or even to decide if the variation among species reflects real biological differences. For this reason, studies employing multiple criteria that can be reliably tested in different species are needed.

This paper is part of a series of studies which seek to elucidate the organization of the visual cortex in *Cebus apella*, a New World (Platyrrhine) monkey. *Cebus* was originally chosen as a model for studies of the New World monkey visual cortical organization due to the fact that it is more readily comparable in many respects to the most intensively studied Old World (Catarrhine) monkey, *Macaca fascicularis*, than the previously employed New World monkey models. First, both the brain size and body size of *Cebus* are similar to those of *Macaca fascicularis*. Thus, allometric effects (Fleagle, 1988) can, to a large extent, be accounted for. Second, the sulcal pattern is, in most individuals, indistinguishable from that of a macaque (Le Gros Clark, 1959). Our previous experience with *Cebus* demonstrates that the position of homologous visual areas in relation to gyral morphology is very similar to that of macaques (Gattass et al., 1987; Rosa et al., 1988; Fiorani et al., 1989). Finally, many aspects of visual behavior such as diurnality, reliance on color vision, skilled use of the hands for foraging, a complex pattern of social interactions (including visual displays as a form of communication), and the absence of extreme dietary specializations link *Cebus* and *Macaca fascicularis* (Fleagle, 1988). On the other hand, we also believe that because *Cebus* is a New World monkey, comparisons with more common Platyrrhine models such as the squirrel monkey, marmoset, and owl monkey can be readily made. Because of this unique combination of characteristics, the study of the *Cebus* monkey may serve as an important link between the models of New and Old World monkey visual cortex.

A model of the organization of the visual areas in the *Cebus* monkey has been described by Sousa et al. (1991), based on previous electrophysiological recordings in V2 and MT and injections of fluorescent tracers in V1. Here, we will describe the areal and laminar patterns of cortical projections to MT. In addition, different patterns of label obtained after injections that invaded MST, an area adjacent to MT, will be described. These anatomical data will be correlated to the myeloarchitecture of the

Abbreviations

6d	cytoarchitectonic area 6, dorsal subdivision
6v	cytoarchitectonic area 6, ventral subdivision
7a	cytoarchitectonic area 7, subdivision a
7b	cytoarchitectonic area 7, subdivision b
7m	cytoarchitectonic area 7, medial subdivision
ArS	arcuate sulcus
CaS	calcarine sulcus
CGp	posterior area of the cingulate gyrus
CMAc	cingulate motor area, caudal subdivision
CoS	collateral sulcus
DI	dorsointermediate area
DLa	dorsolateral anterior area
DLc	caudal subdivision of dorsolateral area
DLi	dorsolateral intermediate area
DLp	dorsolateral posterior area
DLr	rostral subdivision of dorsolateral area
DM	dorsomedial area
DP	dorsal prelunate area
FEF	frontal eye fields
FST	fundus of superior temporal area
HM	horizontal meridian
IOS	inferior occipital sulcus
IPS	intraparietal sulcus
IT	inferior temporal cortex
LaS	lateral sulcus
LIP	lateral intraparietal area
LIPd	lateral intraparietal area, dorsal subdivision
LIPv	lateral intraparietal area, ventral subdivision
LuS	lunate sulcus
M	medial visual area
MIP	medial intraparietal area
MT	middle temporal area
MTc	MT crescent
MST	medial superior temporal area
MST-1	medial superior temporal area, subdivision 1
MST-2	medial superior temporal area, subdivision 2
OTS	occipito-temporal sulcus
PaS	paraoccipital sulcus
PIP	posterior intraparietal area
PO	parieto-occipital area
POd	parieto-occipital dorsal area
POm	parieto-occipital medial area
POmS	parieto-occipital medial sulcus
POS	parieto-occipital sulcus
PP	posterior parietal cortex
STP	superior temporal polysensory cortex
STS	superior temporal sulcus
TEO	cytoarchitectonic area TEO
TVP	temporal ventral posterior area
V1	primary visual area
V2	second visual area
V3	third visual area
V3A	visual area V3A
V3s	third visual area, stratified subdivision
V3*	third visual area, darkly myelinated subdivision
V4	fourth visual area
V4t	transitional V4
VIP	ventral intraparietal area
VM	vertical meridian
VP	ventral posterior area

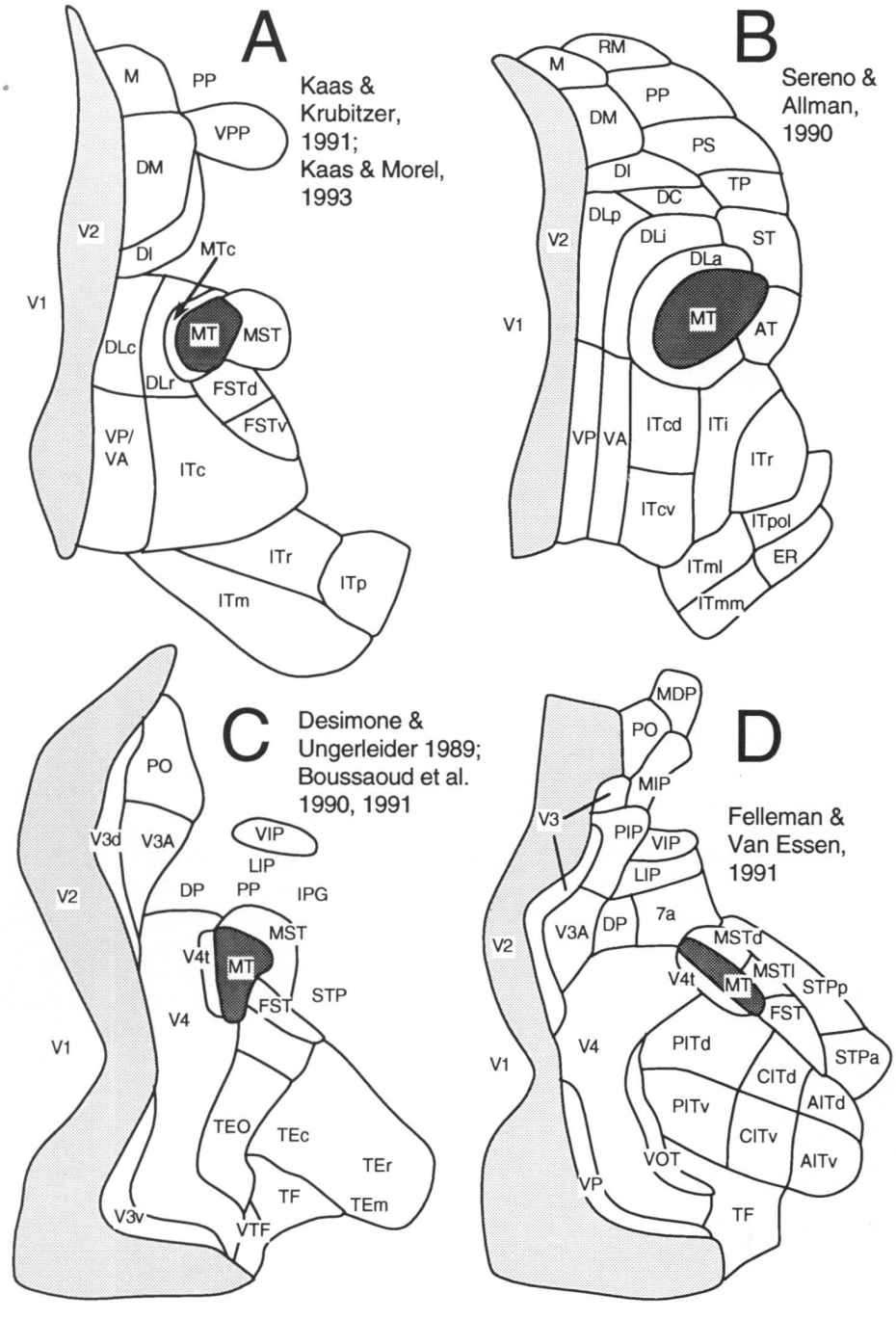

Fig. 1 Different models of the organization of the extrastriate cortex in the owl monkey (A,B) and macaque monkey (C,D), according to recent studies. Each diagram was drawn as a flat reconstruction of a right hemisphere (dorsal upwards; caudal to the left). The location of area V2 is shown in light grey, and that of MT in dark grey. Abbreviations also used in the text are given on page 828; other abbreviations are AITd and AITv: dorsal and ventral subdivisions of anterior inferotemporal; AT: anterior temporal; CITd and CITv: dorsal and ventral subdivisions of central inferotemporal; DC: dorsocaudal; ER: entorhinal; FSTd and FSTv: dorsal and ventral subdivisions of the fundal superior temporal area; IPG: inferior parietal gyrus; ITc inferotemporal, caudal subdivision; ITcd: caudal inferotemporal, dorsal division; ITcv: caudal inferotemporal, ventral division; ITi: intermediate inferotemporal; ITm: inferotemporal, medial subdivision; ITml: medial inferotemporal, lateral division; ITmm: medial inferotemporal, medial division; ITp: inferotemporal polar subdivision; ITpol: polar inferotemporal; ITr: rostral inferotemporal; MDP: medial dorsal parietal; MSTd medial superior temporal dorsal; MSTl: medial superior temporal lateral; PITd and PITv: dorsal and ventral subdivisions of inferotemporal; PS: posterior sylvian; RM: rostomedial; ST: superior temporal; STPa and STPp: anterior and posterior subdivisions of the superior temporal polysensory area; TEc, TEm, and TEr: caudal, medial, and rostral subdivisions of cytoarchitectonic area TE; TP: temporoparietal; V3d and V3v: dorsal and ventral parts of third visual area; VOT: ventral occipitotemporal; VPP: ventral posterior parietal; and VTF: visual subdivision of architectonic area TF.

visual areas of *Cebus*, to provide an updated model of the organization of the extrastriate areas in this species.

Materials and methods

Animal preparation and receptive-field recording

Eight adult male *Cebus apella* monkeys weighing between 1.7 and 4.2 kg were used in this study. In each animal, one injection of the fluorescent tracer Fast Blue was aimed at visual area MT. Out of the eight MT injections, six were later found to be confined to the cortical mantle, and two included MT but spilled out into the white matter. These latter cases were excluded from the analysis. All injections were made under electrophysiological guidance using the visual topography of areas in the superior temporal sulcus (STS) as reference (Fiorani et al., 1989). The experimental procedures for multi-unit recordings were described in detail elsewhere (Rosa et al., 1992). About 10 days prior to the first recording session, under general anesthesia (alphaxalone 10 mg/kg, alphadolone 3 mg/kg, plus ketamine 30 mg/kg initial dose, 10 mg/kg in half-hourly doses), the animal received a cranial prosthesis consisting of a bolt to hold the head in the stereotaxic apparatus in a dental acrylic base. For the recording and injection session, the animal was anesthetized with halothane (2%), followed by a mixture of N_2O/O_2 (7:3). A 12-mm-diameter trephine hole was made in the region over-

lying the STS. Muscular paralysis was then induced by the i.v. injection of 0.1 mg/kg of pancuronium bromide, followed by continuous infusion of the same drug (0.1 mg/kg/h in saline). The continuous infusion solution also included the neuroleptanalgesic sufentanil citrate (2 μg/kg/h). This dose of sufentanil is sufficient to induce a state of light sleep in primates (Lennie et al., 1990). In addition, in the present experiments the anesthetic effect of this drug was enhanced by artificial ventilation with N_2O/O_2 (7:3) through a tracheal cannula during the period of paralysis. The animal's level of expired CO_2, its electrocardiogram, and its rectal temperature were continuously monitored and kept within the normal physiological range. After the application of atropine (2%) and phenylephrine (2%) drops to induce mydriasis and cycloplegia, the eye contralateral to the experimental hemisphere was fitted with a contact lens which focused the eye on the surface of a 57.3-cm-radius transparent hemispheric screen placed in front of the animal. The positions of the fovea and blind spot were projected onto the screen by means of a reversible ophthalmoscope in order to define the vertical and horizontal meridians (VM and HM) of the visual field.

Varnish-coated tungsten microelectrodes were used to record from small clusters of neurons. The microelectrode was advanced through a 21-gauge guide tube, across the dura mater, at 300–500 μm steps. Visual receptive fields were plotted at each site by moving colored bars and, in the case of parietal cortical areas, large textured objects in front of the screen. All stimulation was made under light-adapted conditions. The neuronal activity was monitored using an amplification system connected to a loudspeaker. Changes of neuronal activity were correlated with stimulation of specific portions of the visual field. Maps of the visual topography of areas MT and V4t (transitional V4; Desimone & Ungerleider, 1986; previously referred to as DZ, the "dorsal zone," by Fiorani et al., 1989), as well as changes in the responsiveness, receptive-field size, and stimulus selectivity were used to guide the electrode towards area MT. Since the posterior wall of the STS is nearly vertical in *Cebus*, penetrations were tilted 20–30 deg from the vertical in parasagittal planes in order to avoid labeling of other areas during the withdrawal of the injection syringe (see below). Area MT was readily recognizable by the predominance of direction-selective, brisk neuronal responses to moving stimuli. Area V4t showed receptive fields about the same size as those of MT, but the responses were less brisk and only a minority of sites yielded direction-selective responses. These areas could also be distinguished by the trends in visual topography. In progressively deeper sites along the posterior bank of the STS, receptive fields in V4t move towards the VM in the lower contralateral quadrant, while those in MT move away from the lower VM and may include both the lower and the upper quadrants (Fig. 2). The medial superior temporal area (MST), located anterior and medial to MT, showed much larger receptive fields and brisk responses to fast movement of large objects. Finally, recordings from the fundus of superior temporal area (FST), anterior to MT along the fundus of the STS, were characterized by large receptive fields almost always including the fovea.

Injections of fluorescent tracers

Following recording, injections of Fast Blue (5%) were made with a short bevelled 1-μl Hamilton syringe with a 27-gauge needle. To allow the positioning of the injection in the desired region, the electrode guide tube was advanced through a small slit in the dura mater to within 300 μm of the intended injection site. The electrode was advanced again, so that the retinotopic location of the injection site could be checked. The electrode was then replaced by the syringe and 0.2–0.35 μl of tracer injected at a rate of 0.6 μl/h. The guide tube was left in position for about 30 min after removal of the syringe. This procedure allowed all injections to be positioned in portions of area MT without detectable leakage up the track. However, some injections did spread to adjacent cortical areas or to the underlying white matter.

Histological processing

After variable survival times (20 days typical, 14 days in case 1) the animals, under deep anesthesia (pentobarbitone sodium, 50 mg/kg), were perfused transcardially with normal saline followed by paraformaldehyde [2% in phosphate-buffered saline (PBS)] with increasing concentrations of either sucrose (from 10–30%) or glycerol (from 2.5–10%). These survival times were demonstrated not to result in transneuronal transport, although some leakage to the neuroglia immediately adjacent to the labeled cells was apparent (Conde, 1987). Serial 40-μm-thick sections were obtained using a cryostat. Series of unstained sections, 200 μm apart, were mounted on double gelatinized slides and stored in light-tight boxes. In addition, adjacent series were stained with cresyl violet and for myelin with the Gallyas (1979) and Heidenhain-Woelcke methods. In cases 3 and 6, the Heidenhain-Woelcke method was not used. Instead, a series was stained immunocytochemically with the monoclonal antibody Cat-301 (Hockfield et al., 1983). A full description of the Cat-301 patterns in the visual areas will be the subject of a future publication, and only some points will be mentioned below.

Fig. 2. Left column: Parasagittal sections through the STS, from lateral (A) to medial (D) showing recording sites in MT, MST, FST, V4, and V4t (small dots). Sites are numbered sequentially along the banks of the STS. Zones 0 and 1 of the injection site (Conde, 1987) are shown as concentric zones in section B. Architectonic boundaries are shown as dashed lines. Middle column: Receptive-field centers recorded in the sites shown in the left column. Each diagram is a representation of a portion of the left hemifield with the positions of the VM and HM indicated. Receptive-field centers in MT are shown by filled squares, those in MST by dots, FST by circles, V4 by triangles, and V4t by empty squares. Receptive-field centers belonging to the same area are joined in sequences. Right column: Receptive fields corresponding to the centers shown in the middle column. Fields in MT are shown in different tones of grey (those from section B in dark grey; those from C and D in progressively lighter tones of grey), those in MST in continuous outline, FST in dashed outline, V4 in hatch, and V4t in white. Different scales were used to represent the centers and fields in MST/FST/V4 (upper row) and those in MT/V4t/FST (middle and lower rows).

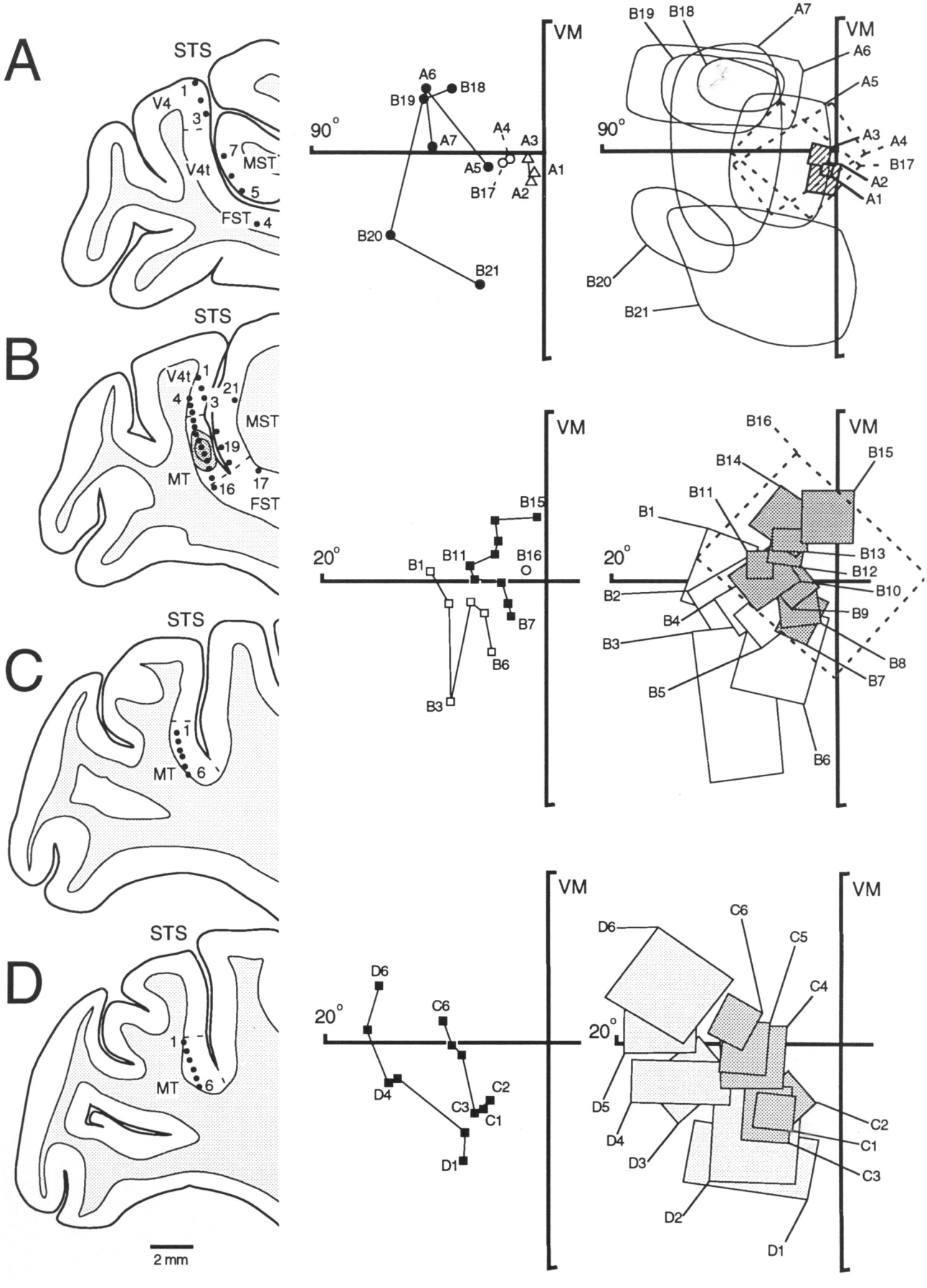
A
STS
V4
1
3
7
MST
V4t
5
FST
4
B
STS
V4t
1
21
4
3
MST
19
MT
16
17
FST
C
STS
1
MT
6
D
STS
1
MT
6
2 mm
VM
90°
A6
B18
B19
A7
A4
A3
A5
A1
B17
A2
B20
B21
VM
B19
B18
A7
A6
A5
90°
A3
A4
B17
A2
A1
B20
B21
VM
20°
B15
B1
B11
B16
B7
B6
B3
VM
B16
B15
B14
B11
B1
20°
B13
B12
B2
B10
B4
B9
B3
B8
B7
B5
B6
VM
20°
D6
C6
D4
C3
C2
C1
D1
VM
D6
C6
C5
C4
20°
D5
D4
D3
C2
C1
C3
D2
D1

FIGURE 2.

Cell plotting, cortical reconstructions, and assessment of the extent of the injections

The unstained sections were scanned with a Zeiss Axioplan fluorescence microscope. This microscope was equipped with a motorized stage, coupled to an IBM-AT microcomputer which ran custom-developed morphometric software. The positions of the labeled neurons and of the injections were then transferred to two-dimensional reconstructions of the neocortex, prepared from the contours of layer IV of sections 1.6 mm apart as described by Van Essen and Maunsell (1980). Architectonic boundaries, as well as the recording sites, were also transferred onto the flattened maps, and used as guides to locate labeled cells with respect to specific areas.

An estimate of the visuotopic extent of the injection site was obtained by examining the location of labeled cells in area V1 and comparing the position of the patches with the visuotopic map described by Gattass et al. (1987). This estimate is shown in outline in the figures corresponding to each case (Figs. 5–10). In addition, the region defined by the borders of receptive fields recorded within the injection site is illustrated for each case (stippled in Figs. 5A–10A, insert). Some mismatch was observed between the recorded receptive fields and the estimates, but this can be accounted for by some individual variability in visual topography of V1 and by the fact that injections usually occupied a larger volume of cortex than that sampled by an electrode penetration. This last factor is particularly important if the small size and low magnification factor of MT are taken into account.

The histological extents of the injection sites were estimated using criteria defined by Conde (1987). The zone containing a deposit of tracer (zone 0) was found to be confined to MT in four out of the six cases. Among these, a second concentric zone containing a halo of tracer interspersed among cells and staining lightly in Nissl preparations (zone 1) was found to encroach upon part of V4t in case 3, and part of MST in case 4. The pattern of label in these cases did not differ significantly from that observed in the other MT cases (1 and 2), therefore supporting Conde's claim that only zone 0 results in retrograde transport. The remaining two cases (5 and 6) showed an involvement of area MST by zone 0.

Identification of visual areas

The primary criterion used for identification of areal boundaries was myeloarchitecture. Delimitation of myeloarchitectonic fields was found to be easier in low-power (5–8×) views of the slides. We used criteria such as the number and degree of separation of myelin-rich and myelin-poor layers, the thickness and position of these layers relative to the pia and white matter, the presence or absence of clear radial bundles of fibers, and the overall intensity of myelination as compared with other areas. In addition, Nissl-stained sections were employed to confirm some boundaries and visualize others that are not clearly evident in myelin-stained material. Some of the architectonic boundaries were confirmed by electrophysiological recordings (Figs. 2 and 4). Descriptions of the architectonic patterns used to identify different areas will be presented in the Results section.

Results

We will start the description of our results by architectonically characterizing the visual areas in *Cebus*. The following sections will deal with the areal, retinotopic, and laminar patterns of connections between these areas and MT, and the effects of involvement of MST in the injection site.

Architectonic characterization of cortical areas

A summary of the cortical subdivisions considered in this paper is shown in Fig. 3. This figure includes areas (such as V1, V2, MT, and PO) whose boundaries were independently confirmed by physiological criteria, as well as others based only on connections and/or architecture. We therefore emphasize the provisional character of some of the boundaries shown in Fig. 3, in so far as previous experience reveals that a single functional area may comprise architectonic subdivisions, and, conversely, that different areas may share a similar architectonic pattern (Sanides, 1972; Tusa et al., 1979; Fiorani et al., 1989; Andersen et al., 1990).

Areas in the STS

Area MT was characterized by its dense myelination relative to surrounding areas, except parts of MST (Allman & Kaas, 1971; Ungerleider & Desimone, 1986*a*; Fiorani et al., 1989). In MT, a thick bundle of fibers extends from layer VI to the bottom of layer III, and the inner and outer bands of Baillarger are obscured by the overall intensity of staining (Fig. 4B). In one animal, a small region of lighter staining (MTp) was also present at the fundus and anterior bank of the STS. Based on physiological studies in *Cebus*, we consider this region an integral part of MT (Fiorani et al., 1989).

Area MST was located adjacent to MT, in the anterior bank of the STS. Most of MST was darkly myelinated, but could be distinguished from MT by the presence of a thick, conspicuous outer band of Baillarger which separates the lower, darkly staining layers from the upper layers (Fiorani et al., 1989). The darkly myelinated subdivision of MST was termed MST-1. By taking into account the connectional data, we found it necessary to expand the architectonic definition of MST in *Cebus* to include transitional regions of less-myelinated cortex in the anterior bank of the STS and in the caudal tip of the lateral sulcus (LaS). The fringe of less-myelinated cortex was termed MST-2 (Fig. 4B).

Area FST (Desimone & Ungerleider, 1986; Fiorani et al., 1989) was characterized by a thin and sharp outer band of Baillarger which separated a broad, myelin-poor upper stratum from a moderately myelinated, nearly homogeneous thin lower stratum. In terms of the overall intensity of myelination, FST was intermediate between darkly staining MT and MST dorsocaudally, and the lighter staining temporal areas anteriorly. FST could also be distinguished from both MST-1 and MST-2 by the thickness and relative depth of the outer band of Baillarger. In FST, this band was thinner and closer to the white matter than in MST.

Area V4t in *Cebus* could be distinguished from V4, posteriorly, by the absence of the lightly myelinated band between the inner and the outer bands of Baillarger, and from MT by the presence of a darkly stained sharp outer band of Baillarger (Fig. 4B). The density of myelination decreased from lateral to medial portions of this area. Complementing our previous observations (Fiorani et al., 1989), we were able to demonstrate that V4t borders the foveal representation of MT, and possibly a small portion of the upper quadrant representation.

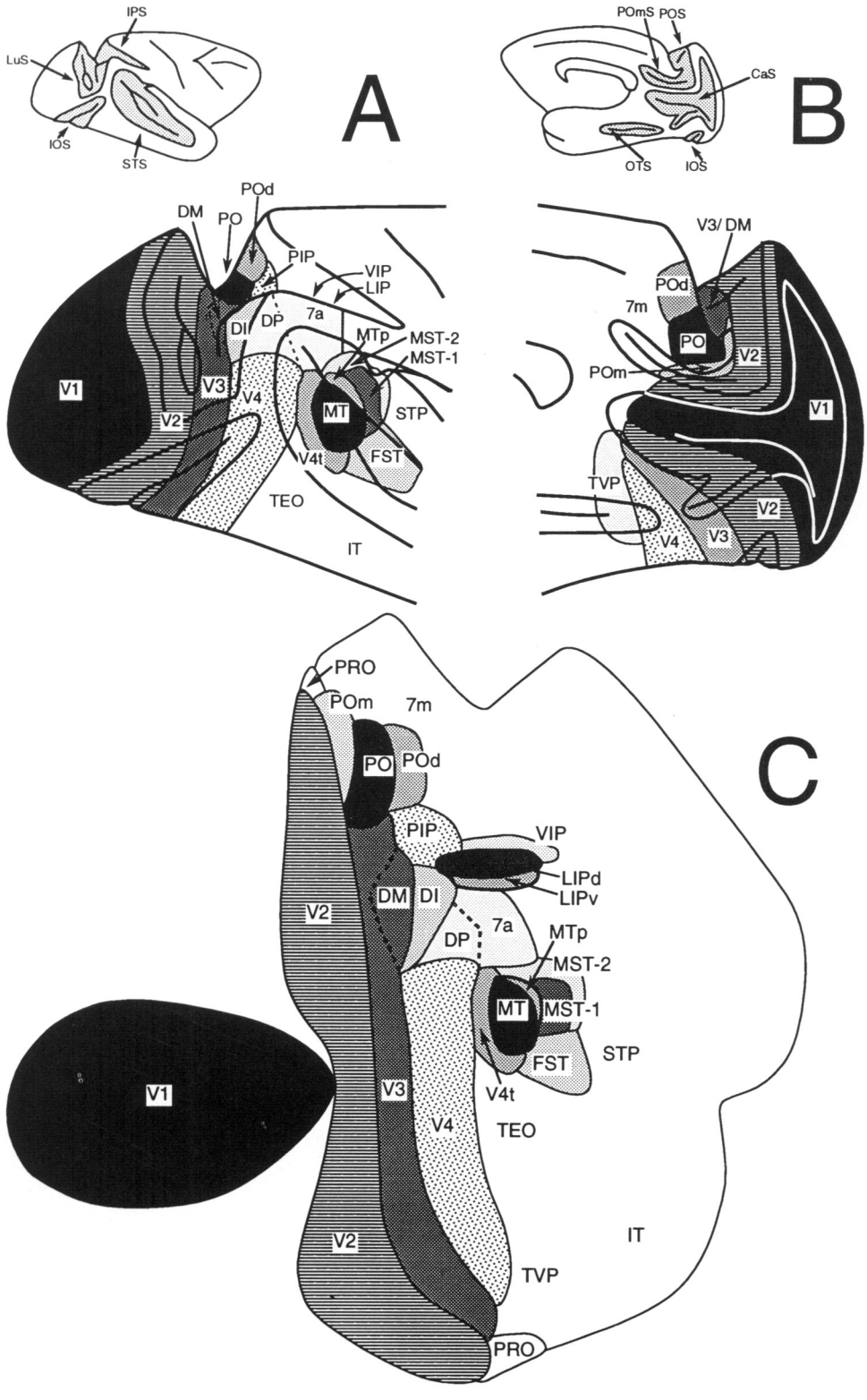

Fig. 3. Architectonic subdivisions of the extrastriate cortex in the *Cebus* monkey. Upper: Lateral (A) and medial (B) views of a right hemisphere of a *Cebus* monkey, with the sulci partially opened. These diagrams are based on photographs of a brain in which the sulcal banks were physically retracted. The upper inserts in A and B show full views of the cerebral hemispheres, with the cortex hidden by the sulci in grey and the major folds in continuous line; the lower portions show enlarged views of the posterior half of the brain, with the approximate location of architectonic fields shown by different types of stipple and fill. C: The same subdivisions shown in A and B are displayed in a schematic flat map of a right hemisphere. This map incorporates features of all cases, and therefore does not correspond to any specific animal. Dashed lines show borders that were estimated on the basis of physiological evidence, but could not be observed in myelin-stained sections.

Areas V3, DM, and DI

Anatomical tracer studies (Sousa et al., 1991) and electrophysiological recordings in *Cebus* (Gattass et al., 1988*b*; and in preparation) showed that V2 is bordered anteriorly by an area homologous to the macaque's V3 (Gattass et al., 1988*a*). The myeloarchitecture of V3 presented two alternating patterns, which we refer to as V3s (stratified) and V3*. In the V3s pattern, the outer band of Baillarger was more sharply defined than in V2, allowing the determination of the V2/V3 boundary (Fig. 4A). Stratified V3 was further characterized by moderate to dark myelination, a sharp limit between the outer band and the upper layers, and fuzzy pale bands located between the two bands of Baillarger and between the inner band and the white matter. The subdivision V3*, named after the possible

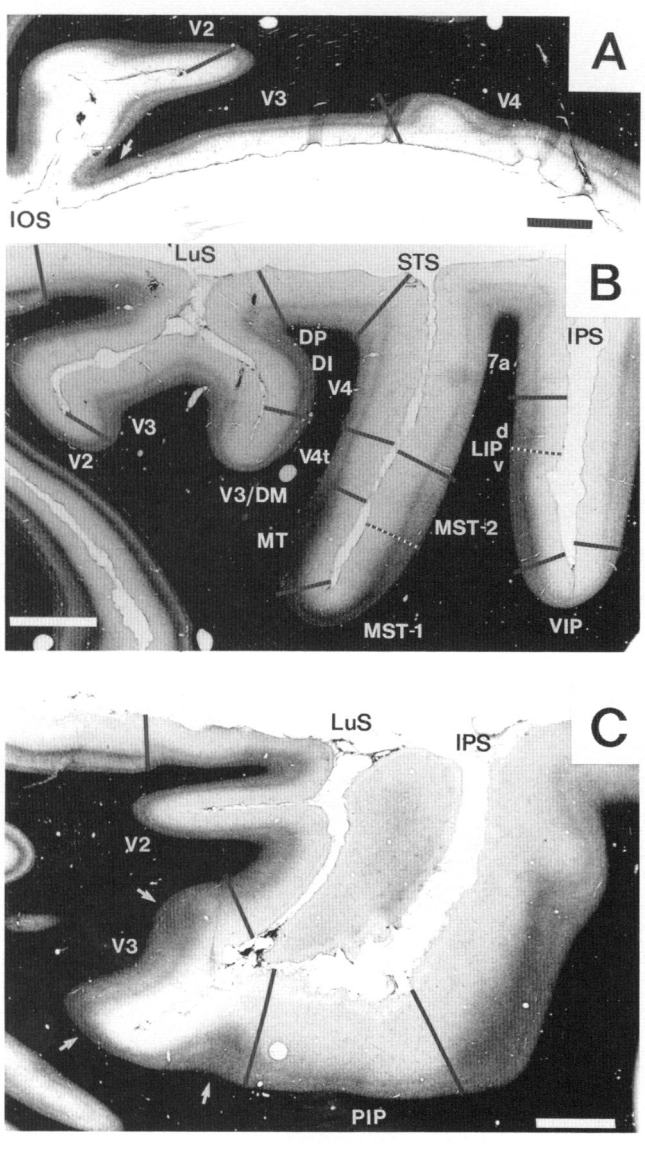

Fig. 4. Myeloarchitecture of the occipital lobe and adjacent cortex in *Cebus*. In each panel, anterior is to the right, dorsal is upwards, and the scale bars correspond to 2 mm. The thick black lines across cortical layers mark the center of the transition between cortical areas, the dashed lines mark the boundaries between architectonic subdivisions of a given area, and the arrowheads in A and C point to the darkly myelinated (V3*) patches in V3. Some electrode tracks are also visible.

homologue in the macaque (Van Essen et al., 1986), was characterized by darker myelination overall and less clearly separated bands of Baillarger than in V3s (Fig. 4C). Although most of V3 was formed by the V3s pattern, V3* consisted of islands within the stratified pattern. These islands were more commonly, but not exclusively, found in the peripheral representation of the lower quadrant, in the annectent gyrus and in the parieto-occipital cleft (Fig. 4C). Based solely on the density of myelination, V3 could not be reliably separated from V2. V3s was at least as myelinated as the central representation in V2, and V3* was similar to the peripheral representation in V2 (Rosa et al., 1988). Thus, laminar patterns must also be taken into consideration. In contrast to the situation in the macaque (Fig. 1), there was no evidence for a gap at the foveal representation separating the upper and lower quadrant representations in V3.

Electrophysiological recordings in *Cebus* monkeys (Gattass et al., manuscript in preparation) suggest that V3 is bounded anteriorly in the annectent gyrus by another area containing representations of both the lower and upper visual quadrants. This area probably corresponds to the dorsomedial visual area (DM) described in owl monkeys (Allman & Kaas, 1975) and area V3A of the macaque (Zeki, 1978; Gattass et al., 1988*a*). For reasons of historical precedence, we favor the first nomenclature. We were unable to distinguish V3 from DM based on myeloarchitecture. The architectonic field DI (dorsointermediate area; Allman & Kaas, 1975; Krubitzer & Kaas, 1990) comprised cortex anterior to V3/DM and posterior to the dorsal prelunate area (DP), mostly in the anterior bank of the paraoccipital sulcus (PaS). The main myeloarchitectonic feature of DI was the broad and heavily stained outer band of Baillarger (Fig. 4B). The lower layers were more densely myelinated than in DP and poorly differentiated.

Areas V4, TEO, and TVP

The myeloarchitectonic characteristics of V4 in *Cebus* closely resemble those in the macaque (Gattass et al., 1988*a*). These include a moderate degree of myelination, sharply defined bands of Baillarger, and a crisp light band separating them (Figs. 4A and 4B). Separation of V3 and V4 was made possible by the lighter myelination and by the much clearer separation between the bands of Baillarger in V4 (Fig. 4A). The anterior limit of V4 with area TEO (Von Bonin & Bailey, 1947) was characterized by a further decrease in overall myelination and an even clearer separation between the bands of Baillarger (Boussaoud et al., 1991). The temporal ventral posterior area (TVP; Sousa et al., 1991) was characterized by thin, lightly myelinated cortex and sharp bands of Baillarger. TVP was mostly included in cytoarchitectonic area TF (Von Bonin & Bailey, 1947).

Areas 7a and DP

In *Cebus*, areas 7a and DP were architectonically similar to those same areas defined in the macaque (Andersen et al., 1990). In myelin-stained sections they were characterized by light myelination, a sharp outer band of Baillarger, and a lower stratum showing clear radial bundles of fibers and little separation between the layers (Fig. 4B). A light band separating the inner and outer bands of Baillarger was not conspicuous in these areas. This characteristic was useful in defining the ventral boundary of DP, as in V4 the light band was clearly defined. In our anesthetized preparations, we were often able to plot receptive fields in DP, but not in 7a. We could not reliably separate DP from 7a using architectonic criteria, and their boundary is estimated by analogy with the macaque (Andersen et al., 1990).

Areas in the intraparietal sulcus (IPS)

The lateral intraparietal (LIP) and ventral intraparietal (VIP) areas were defined in the *Cebus* using the same architectonic criteria as Blatt et al. (1990) in the macaque. Area LIP, in the lateral bank, was formed by two subdivisions. The subdivision LIPv (LIP ventral Fig. 4B) had a matted appearance in myelin-stained sections, with fibers extending from layer VI to the bottom of layer III. Its dark myelination contrasted with that of cortex located more dorsally in the ventral bank of IPS, which showed the same pattern as area 7a. However, this transition was not sharply defined, extending over a strip of cortex about 2 mm wide. Since the transitional region was also found to project to MT, it was considered an integral part of LIP, and

named LIPd (LIP dorsal) according to Blatt et al. (1990). A lightly myelinated region located around the fundus of the IPS was considered to be area VIP (Fig. 4B; see also Andersen et al., 1990; Colby et al., 1993).

The parieto-occipital area (PO; Colby et al., 1988) was located in the ventral portions of the medial wall of the IPS and the anterior wall of the parieto-occipital sulcus (POS), as well as in the precuneate gyrus. PO had a darkly myelinated, matted pattern similar in all aspects to that of MT, which contrasted with the surrounding areas (Neuenschwander, 1989; Neuenschwander et al., submitted). Area POd corresponds to a second representation of the peripheral visual field, dorsally adjoining that of PO (Neuenschwander, 1989; Gattass et al., 1990). In our material, POd was not as heavily myelinated as PO. However, it stained darker than either the dorsally adjoining caudal subdivision of the somatosensory association cortex (area PE of Von Bonin & Bailey, 1947) or laterally adjoining posterior intraparietal (PIP) cortex. Based on its location and architecture (Colby et al., 1988), PIP corresponded to a lightly myelinated region located at the fundus and medial bank of the posterior portion of the IPS. This area had thin and well-separated bands of Baillarger (Fig. 4C).

Area POm

Evidence for a further visual area in the PO complex, adjacent to the dorsal tip of V2, was obtained in *Cebus* by Neuenschwander (1989), based on receptive-field mapping. This area was called POm, since it crosses both banks of the medial parieto-occipital sulcus (POmS). The myeloarchitectonic differences between V2 and POm were subtle. The distinction between these areas was possible in some cases due to the more clearly separated bands of Baillarger and lighter myelination in the latter. In most animals, however, the border between V2 and POm was estimated based on physiological studies in other animals and topographic and laminar distribution of labeled cells, which differed from those in V2.

Areas in the arcuate sulcus

The subdivisions of the frontal cortex relevant to this study were more easily distinguished in low-power views of Nissl-stained sections. A cytoarchitectonic boundary roughly coincident with the fundus of the arcuate sulcus (ArS) marked the border between the frontal eye field (FEF), anteriorly, and premotor area 6, posteriorly. In FEF, the granular layer IV was visible, while in area 6 it was not (Bruce et al., 1985). The characteristics of layer IV were also used to mark the anterior border of FEF, close to the lip of the ArS. In anteriorly located areas, this layer was sharply defined, while in FEF it was broad and fuzzy. In the posterior bank of the ArS, a border between dorsal (6d) and ventral (6v) premotor areas was drawn based on myeloarchitecture. The dorsal subdivision was densely myelinated, while the ventral subdivision was lighter and had visible bands of Baillarger.

Regional and laminar distribution of labeled neurons

Figs. 5–10 illustrate the regional distribution of labeled cells after four injections in area MT (Figs. 5–8), and two injections involving areas MT and MST (Figs. 9–10).

Areas V1 and V2

The pattern of projections to MT from both V1 and V2 followed visuotopic constraints, i.e. only the parts representing the same portion of the visual field were connected. This topography can be observed in V1 by comparing the location of label in cases 1, 2, and 5, which form a central-peripheral series. Although the injection in the central (5 deg) representation in case 1 resulted in label mainly in the occipital operculum (Fig. 5), the labeled patches in V1 in case 2 (injection at 10 deg; Fig. 6) and case 5 (injection in the peripheral representation; Fig. 9) are progressively more anterior in the calcarine sulcus (CaS) (to the left, in the flat reconstructions). Cases 3 (Fig. 7) and 6 (Fig. 10), in spite of the imprecision due to the invasion of MST in the latter, are illustrative of the distribution of label after injections in the lower and upper quadrant representations in MT, respectively. In the case with lower quadrant injection (Fig. 7), the location of label in V1 (and also V2) corresponded to the receptive fields recorded in MT but not to the V4t receptive fields. Finally, in case 4 (Fig. 8) the deposit of tracer involved both the upper and lower quadrant representations in MT, and two labeled patches were found in V1 in the expected locations. The vast majority of labeled cells in V1 were found in layer IVb; only a few labeled cells were seen in infragranular layers. This laminar distribution was constant irrespective of invasion of MST by the injection.

Retinotopic order could also be observed in the connections between V2 and MT. The existence of label in both the dorsal and ventral portions of V2 in the cases with injections restricted to MT (Figs. 5–8) reflected the inclusion of the representation of the HM in the injection site. However, in case 1 there was a pronounced bias in the distribution of label towards ventral V2, as expected from the receptive fields recorded at the center of the injection (Fig. 5). In contrast, an injection in the lower quadrant in MT resulted in strong label in dorsal V2 (case 3, Fig. 7). The cases with MST involvement were more difficult to interpret, as this may have resulted in considerable label in peripheral V2 (Boussaoud et al., 1990). For example, in case 6 (Fig. 10) label in V2 reached the far peripheral representation in the anterior portion of the ventral bank of the CaS, in spite of the fact that the receptive fields recorded in MT and the label in V1 were compatible with a mid-peripheral injection. Nonetheless, this injection resulted in label almost exclusively in ventral V2, as appropriate for an upper quadrant injection. In case 5 (Fig. 9), the peripheral parts of both dorsal and ventral V2 were labeled.

In every case, serial reconstructions demonstrated that label in V2 was located in a series of elongated patches, reminiscent of the cytochrome-oxidase stripes described by Tootell et al. (1983), with virtually no labeled cells between the patches. This characteristic of the V2-MT projection was expected, by analogy with previous work in other primates (De Yoe et al., 1990; Krubitzer & Kaas, 1990). Label in V2 was predominantly supragranular. Labeled cells were scattered at all levels of layer III, but were more strongly concentrated in the lower half of this layer. Infragranular labeled cells were more frequent than in V1.

Areas V3, V4, and DM

Considering first the representation of the upper quadrant in the ventral part of V3, a clear topography was present. After an injection in the central upper quadrant representation (case 1, Fig. 5), label in V3 was predominantly located in the inferior occipital sulcus (IOS) and adjacent tentorial cortex. In successively more peripheral injections, (Figs. 6, 8, and 9), the patches of label were displaced anteriorly and away from the IOS. Injections restricted to the vicinity of the HM representation resulted

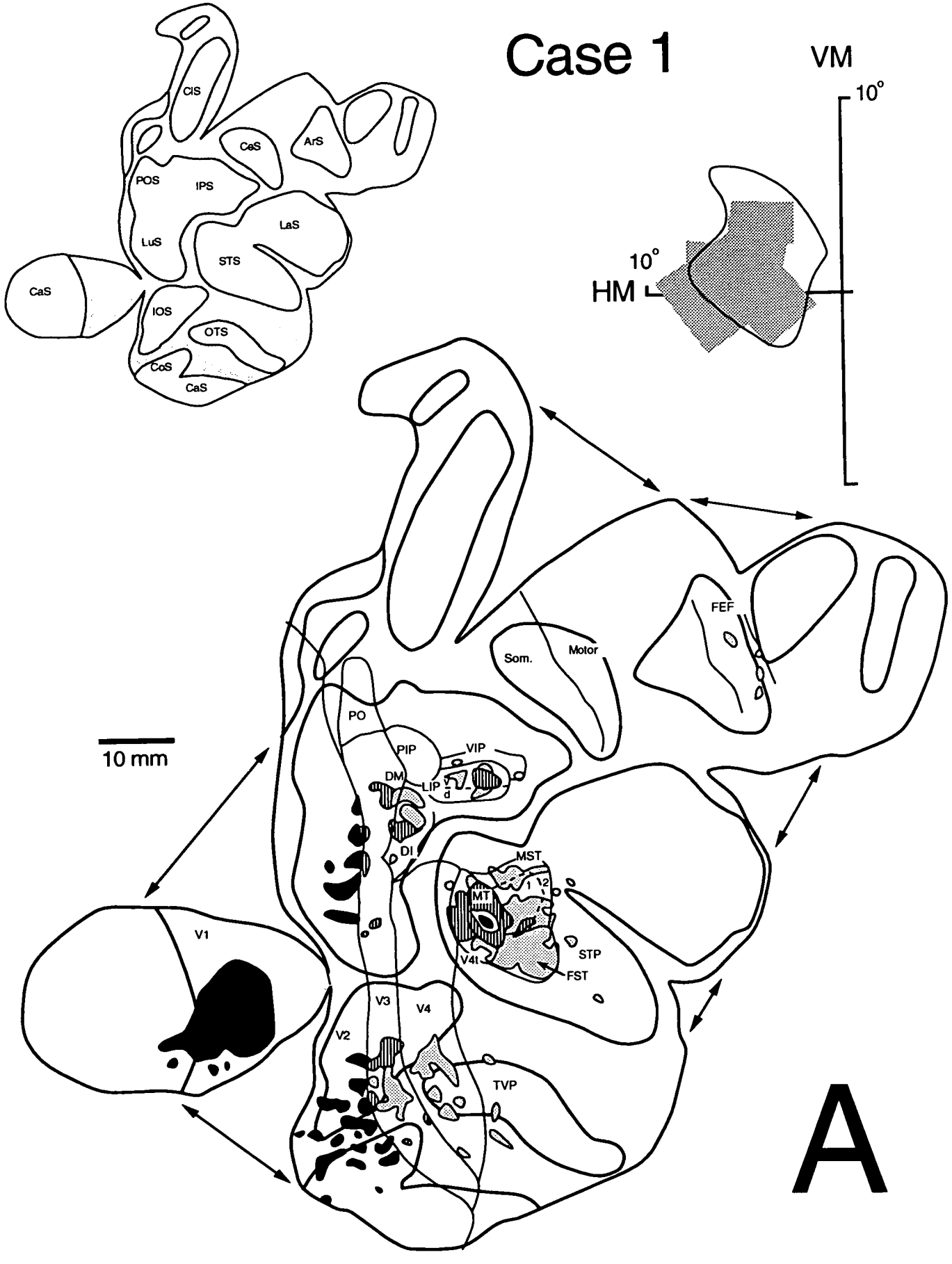
Case 1
VM
10°
10°
HM
CIS
CeS
ArS
POS
IPS
LaS
LuS
STS
CaS
IOS
OTS
CoS
CaS
FEF
Som.
Motor
PO
PIP
VIP
DM
LIP
d
DI
MST
MT
1
2
V1
STP
V4t
FST
V3
V4
V2
TVP
10 mm
A

FIGURE 5A.

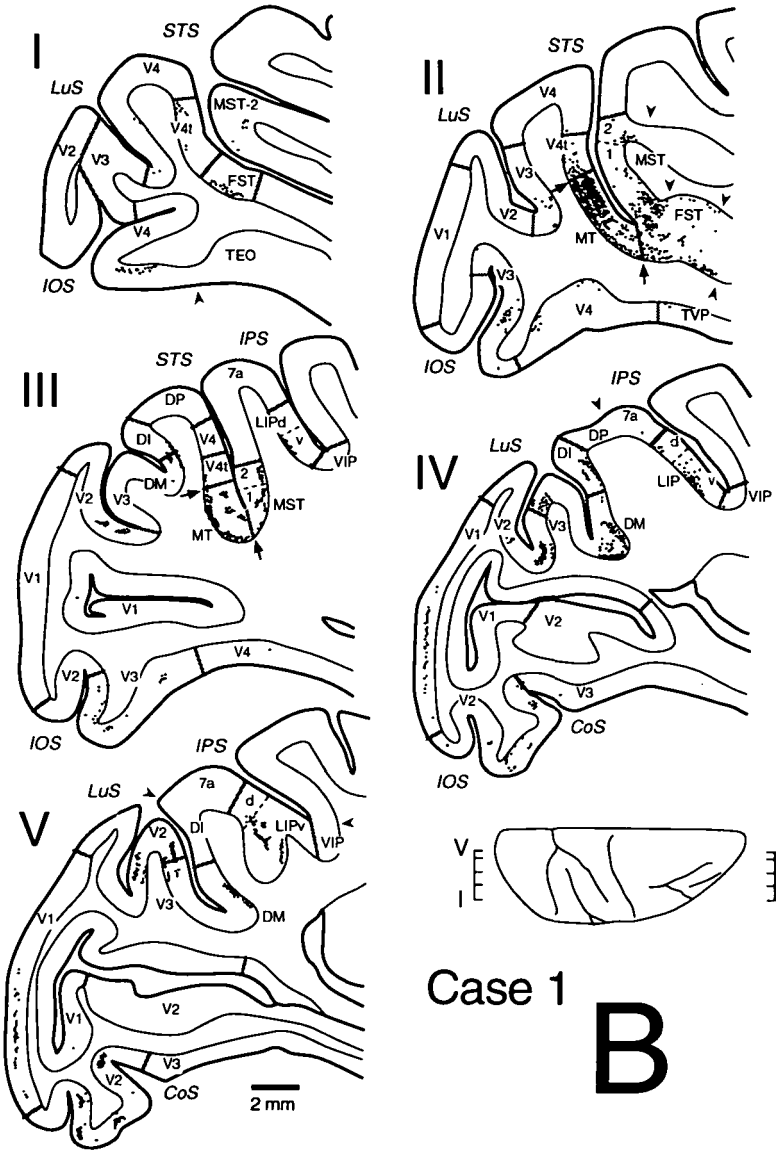

Fig. 5. Summary of data from a case with injection of Fast Blue in the central representation in MT. The deposit of tracer was centered on layer IV, but included layers II to VI, as evaluated by examination of serial sections. Part A: Upper left: flat reconstruction of the right neocortex, showing the gyral (grey) and sulcal (white) regions. Upper right: Representation of the central visual field showing the estimated visuotopic extent of the injection site, determined as explained in "Materials and Methods" (outline), and the receptive fields recorded at the injection site (grey). Lower: Flat reconstruction of the neocortex showing the distribution of label after an MT injection (in MT, black indicates the effective injection site, and white the halo). Discontinuities were made in the process of preparing the flat reconstruction, and the large arrows point to homologous points on the two sides of the discontinuities. In this and in the following figures,the following conventions apply: thick lines limit the neocortex and indicate the sulcal boundaries; thin lines are areal boundaries; dashed lines are architectonic boundaries between subdivisions of a single area (LIPd and LIPv; MST-1 and MST-2); black fill: predominantly supragranular projection patches; vertically striped fill: mixed infragranular and supragranular projection patches; light grey: predominantly infragranular projection patches. Scale bar is uncorrected for shrinkage. Single neurons occasionally found outside the main projection patches are not shown in part A, but may appear in part B. Part B: Sections from the same case, showing the laminar location of the labeled cells. I–V are parasagittal sections at the levels shown in the dorsal reconstruction (lower right). Architectonic boundaries between areas are shown in thick grey line across the cortical layers, and architectonic limits between subdivisions of a single area by dashed lines across the cortical layers. The borders of MT are emphasized by arrows. Boundaries that could not be directly visualized in the sections are estimated (arrowheads). Only the cortical projections are shown.

in a concentration of label close to the V2 border (Figs. 6, 8, and 9), while injections also involving the vicinity of the upper quadrant VM representation resulted in a more even distribution of projecting cells across the width of V3 (Figs. 5 and 10). Finally, an injection largely restricted to the lower quadrant representation resulted in only a few labeled cells at the ventral V2/V3 border (Fig. 7).

The pattern of label in the cortex anterior to dorsal V2 was more complex, although a crude central-peripheral gradient was observed. In the case where the peripheral representation in MT

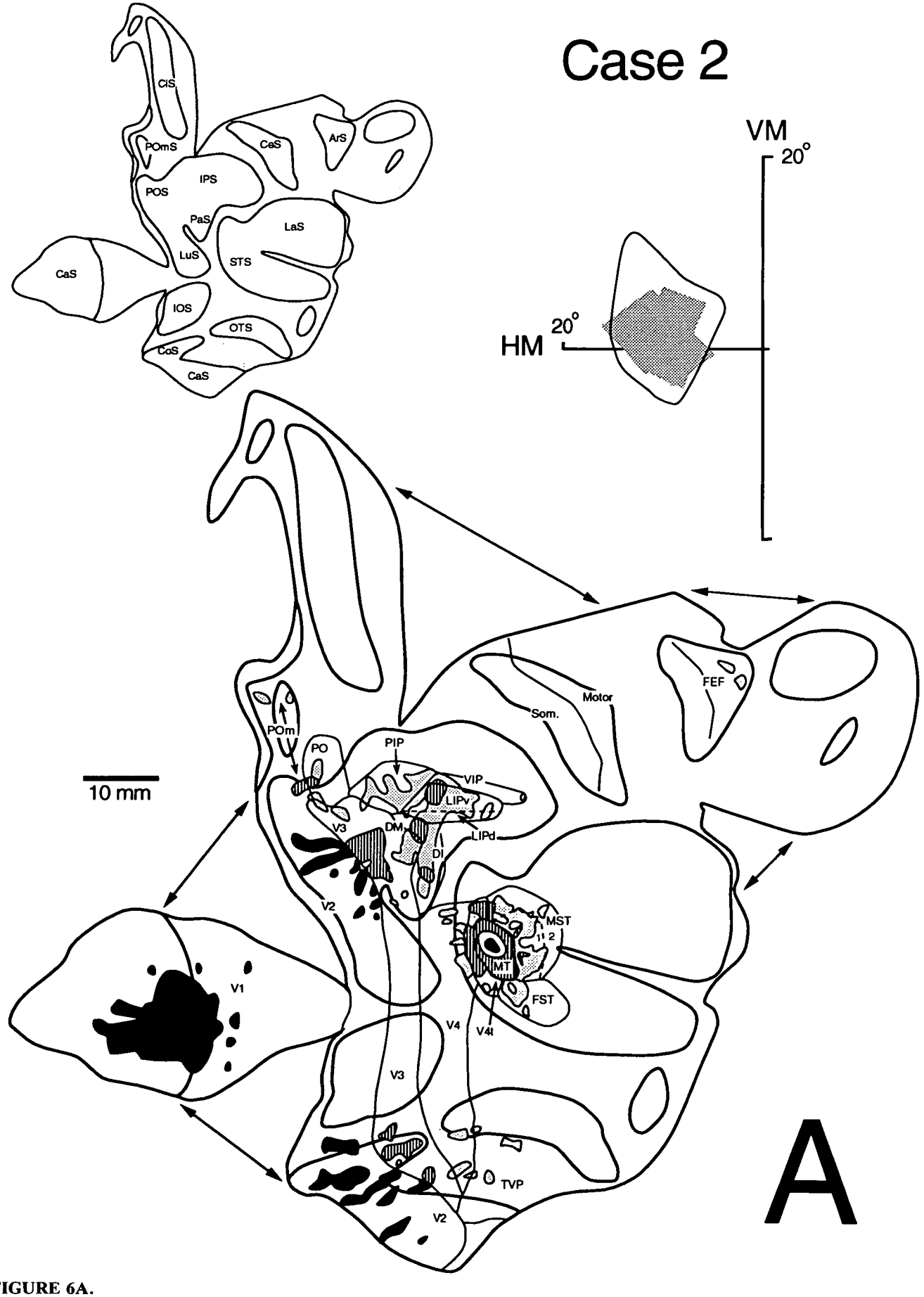
Case 2
VM
20°
HM
20°
CiS
POmS
CeS
ArS
IPS
POS
PaS
LaS
LuS
STS
CaS
IOS
OTS
CoS
CaS
10 mm
POm
PO
PIP
VIP
LIPv
LIPd
V3
DM
DI
V2
MST
MT
FST
V1
V4
V4t
V3
TVP
V2
Som.
Motor
FEF
A

FIGURE 6A.

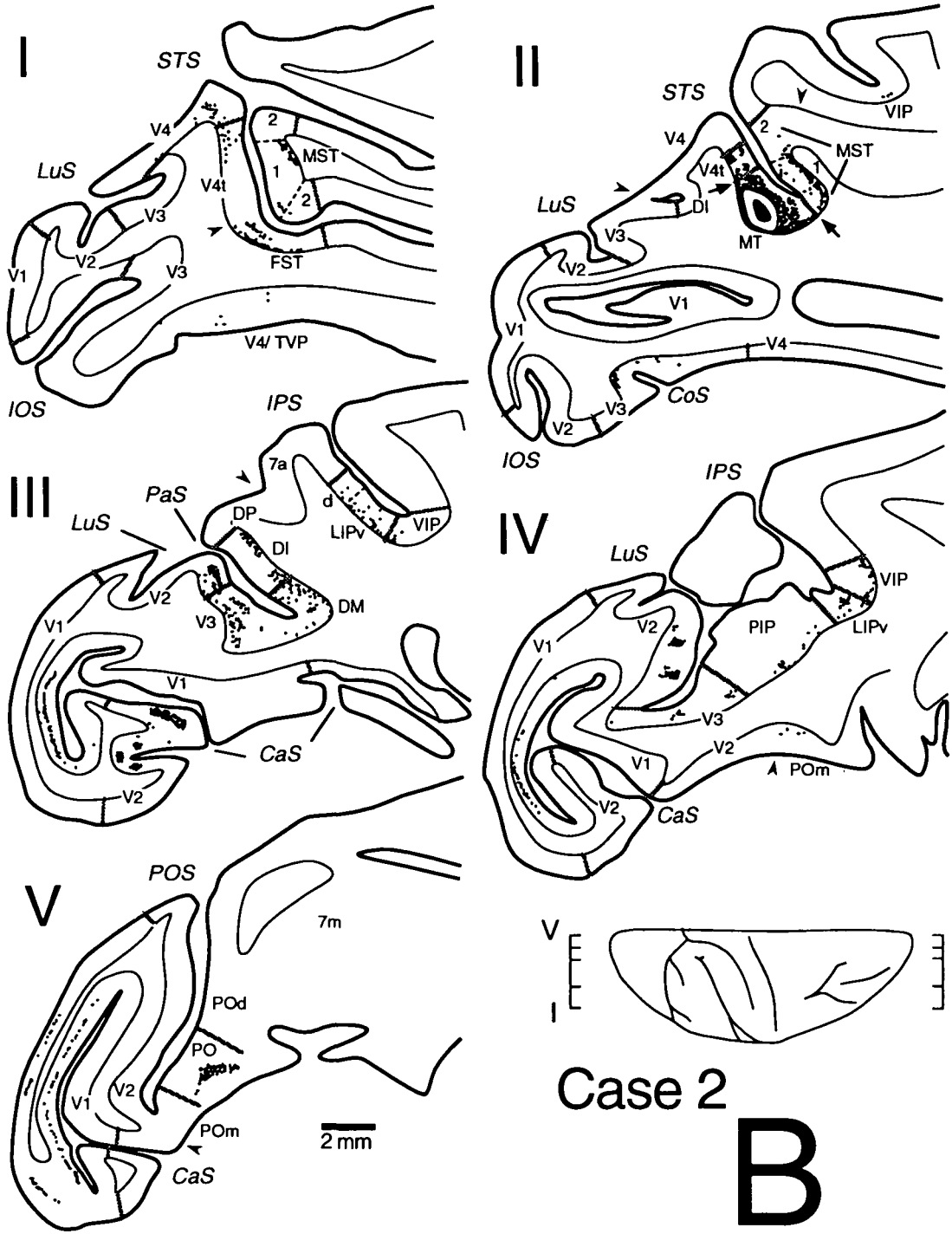

Fig. 6. Summary of data from case 2. Injection involved layers III to VI in MT. Conventions are as in Fig. 5.

was injected, label in V3 extended medially to the border of area PO (Fig. 9), while in the case in which the central representation was injected the label was several millimeters away from this border (Fig. 5). However, in most cases label was widespread along the medio-lateral dimension, and usually included both myeloarchitectonic subdivisions of V3, as well as cortex that may belong to area DM. Moreover, a separation between representations of HM and VM was not apparent. Patches of label usually occupied the whole anterior-posterior dimension of the V3/DM region. In general, these observations agree with the hypothesis of two areas in this region, resulting in a more complex visual topography.

The interpretation of the retinotopy in V4 was relatively straightforward. Firstly, there is evidence for a large emphasis on central representation, as illustrated by the many dense patches of label in V4 in case 1 (Fig. 5) and by much less-extensive label in V4 after injections in the peripheral representation (e.g. Figs. 6, 8, and 9). Secondly, a central-peripheral gradient from lateral to anteromedial was present, with the lower and upper visual-field peripheries represented in the posterior bank

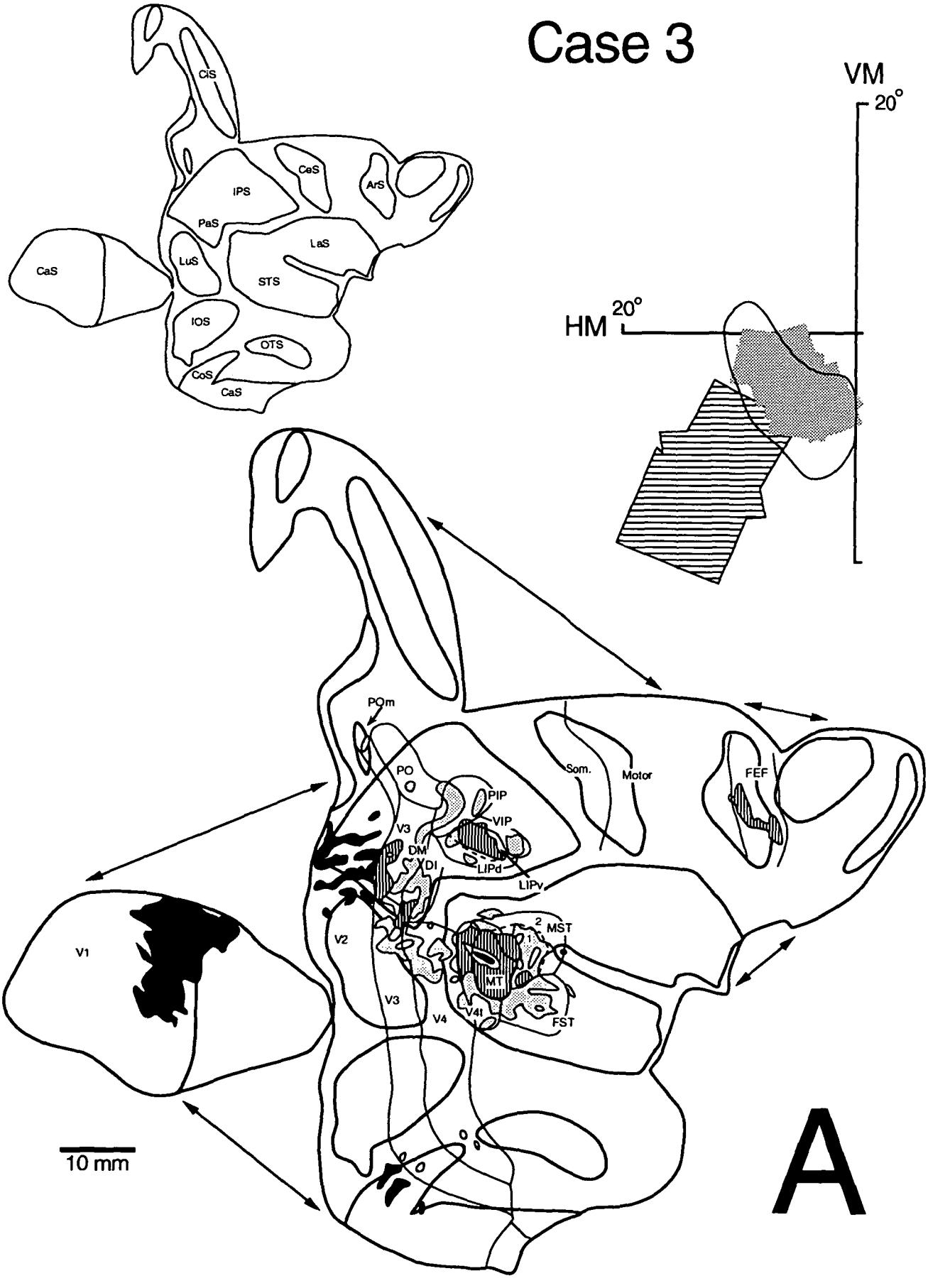
Case 3
VM
20°
HM
20°
CiS
CaS
IPS
CaS
ArS
PaS
LaS
LuS
STS
IOS
OTS
CoS
CaS
POm
PO
PIP
VIP
V3
DM
DI
LIPd
LIPv
Som.
Motor
FEF
V1
V2
V3
V4
V4t
MT
MST
FST
10 mm
A

FIGURE 7A.

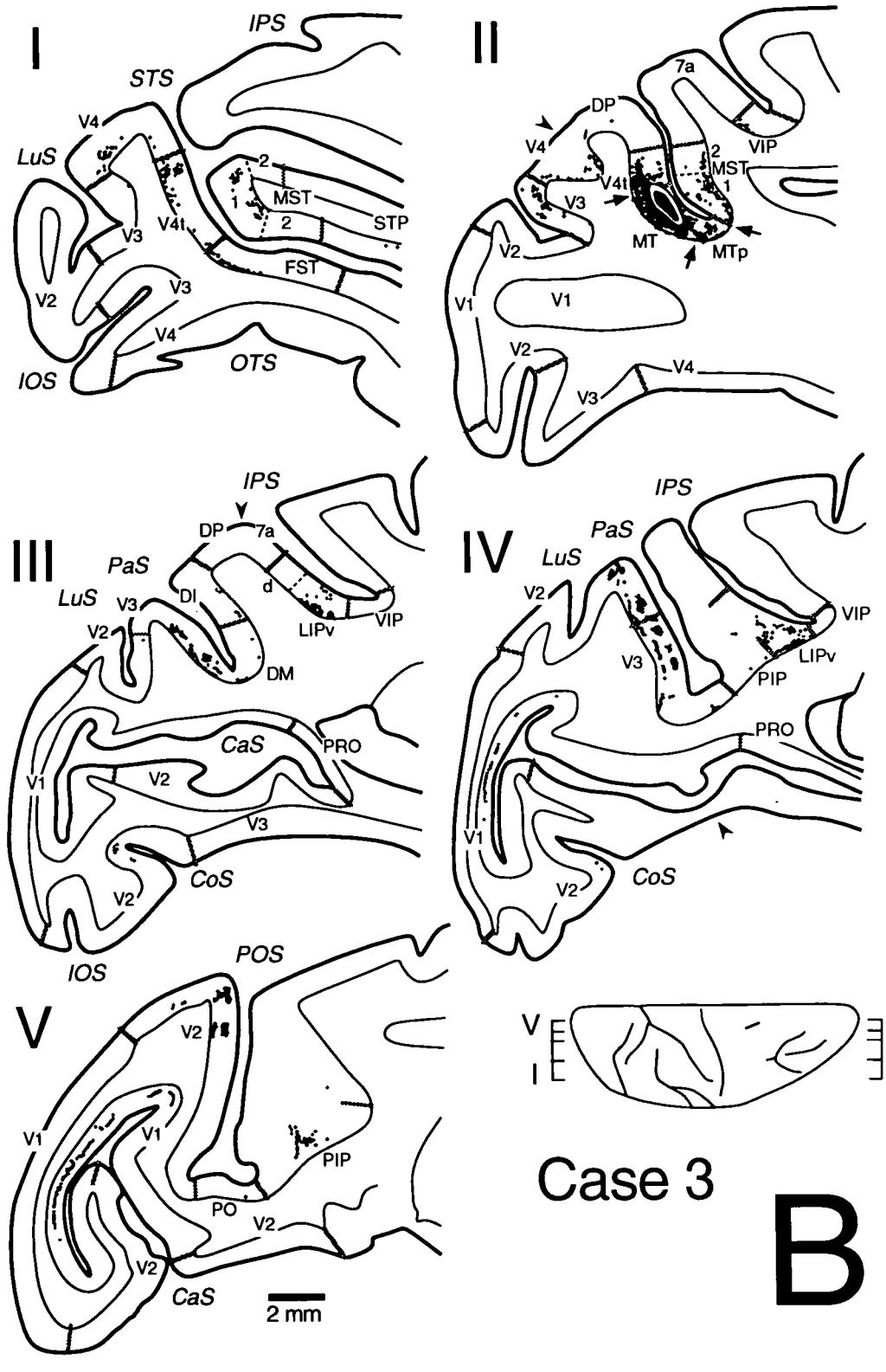

Fig. 7. Summary of data from case 3. Injection involved layers II to VI in MT. In the upper right portion of A, receptive fields recorded along the same electrode track in MT (grey) and V4t (horizontal hatch) are compared with the estimate of the effective site (outline). Other conventions are as in Fig. 5.

of the STS and ventral to the medial lip of the OTS, respectively. Thirdly, the representation of the VM seemed to lie posteriorly (Fig. 8), and that of the vicinities of the HM anteriorly (other cases). The near absence of label in dorsal V4 in the case shown in Fig. 5 may also indicate that, as in the macaque (Gattass et al., 1988*a*), the portions of the lower quadrant close to the HM were represented in the anterior part of ventral V4, rather than in the STS.

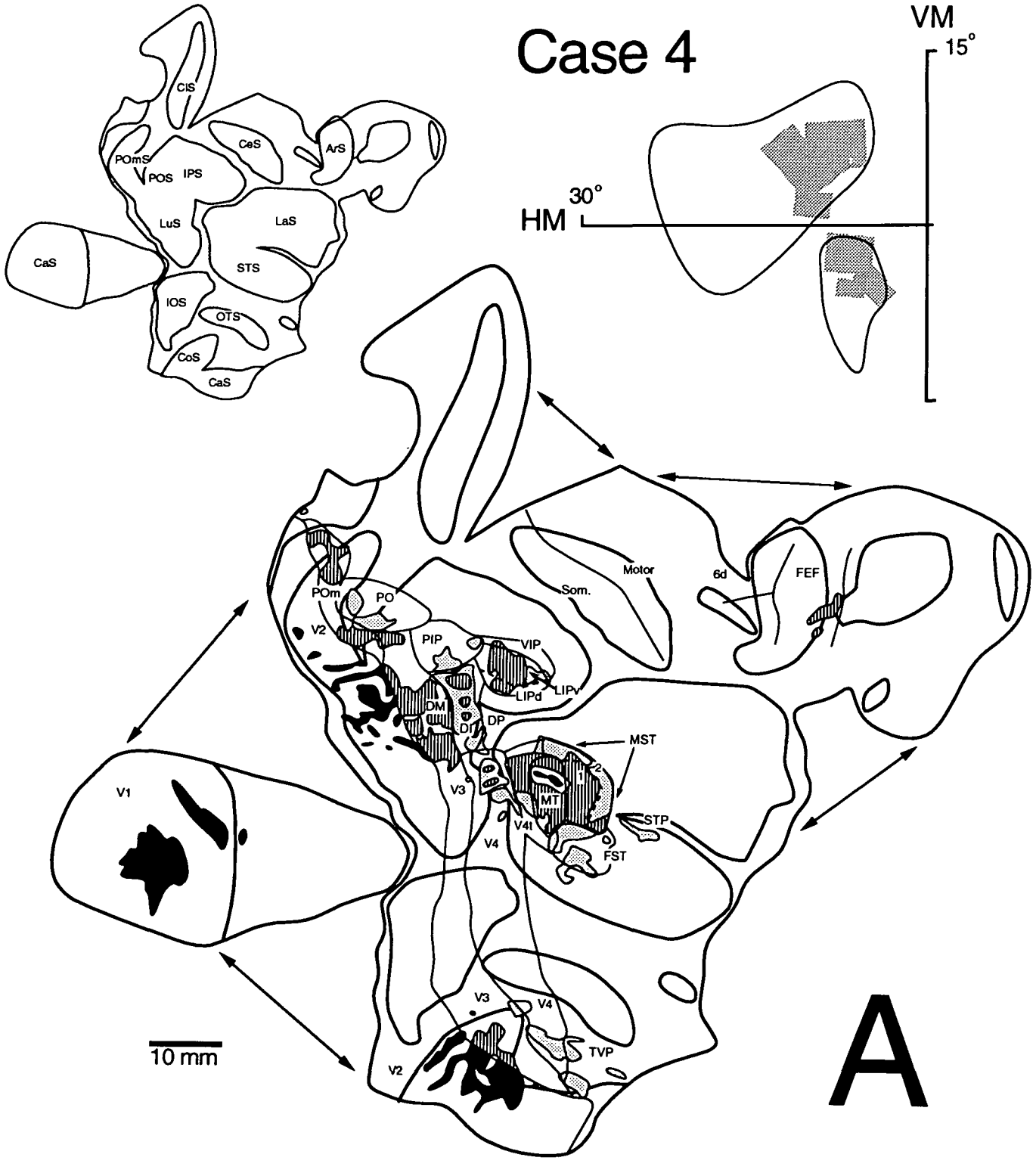

FIGURE 8A.

In every case, label in V3, DM, and V4 consisted of isolated patches, with few if any labeled cells in between. There were, however, clear differences between the laminar distribution of label in these areas. Patches of label in V3 and DM often showed a prominent supragranular component in addition to widespread infragranular label, while in V4 nearly all labeled cells were in infragranular layers.

Area DI

The label in DI included mainly infragranular neurons but some "hot spots" containing densely packed labeled supragranular neurons were observed. The supragranular contribution was substantially larger in the case with extensive MST involvement (Fig. 10). The widespread nature of the label in each case suggests a crudely topographic or non-topographic organization.

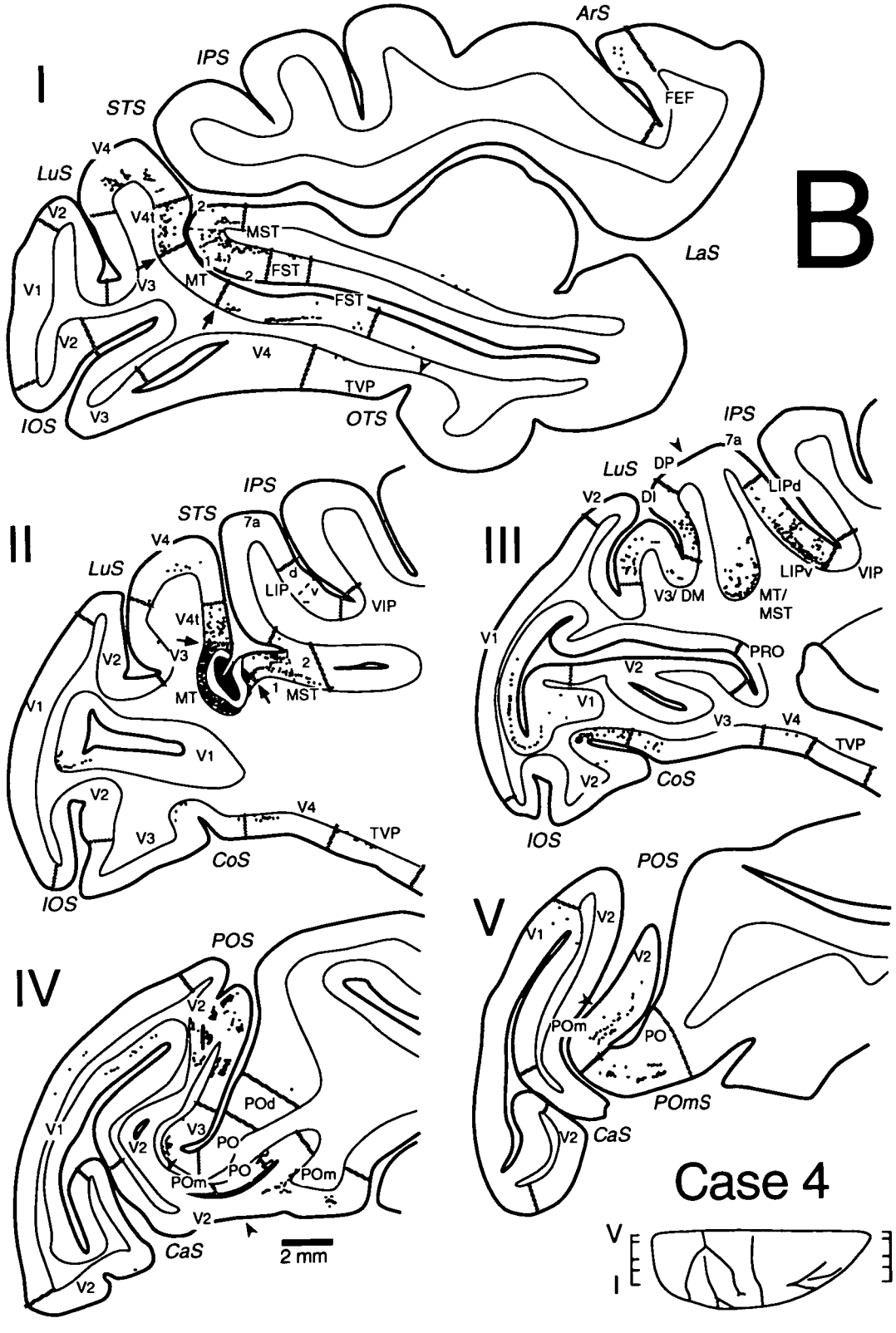

Fig. 8. Summary of data from case 4. Injection involved layers I to V in MT. Conventions are as in Fig. 5.

Areas MST, FST, V4t, and STP

Extensive label was observed in MST, without clear topographic order. Within the labeled regions, cells in MST were nearly continuously distributed in the infragranular layers, but were grouped in small patches in the supragranular layers. No supragranular label was found in the MST-2 subdivision, with the exception of the case with extensive MST-1 involvement (Fig. 10).

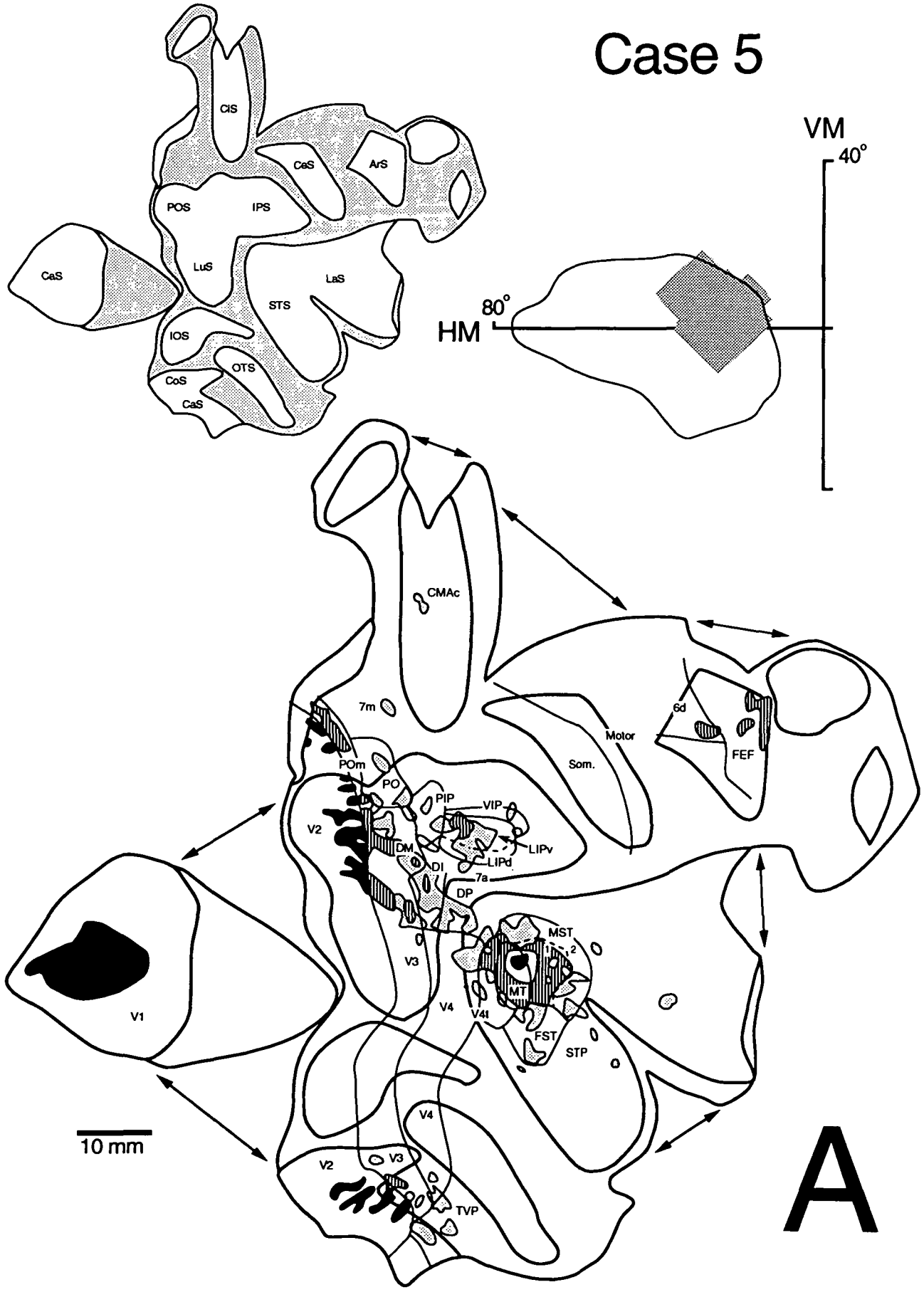
Case 5
VM
40°
HM
80°
CIS
CeS
ArS
POS
IPS
CaS
LuS
LaS
STS
IOS
OTS
CoS
CaS
CMAc
7m
6d
Motor
Som.
FEF
POm
PO
PIP
VIP
V2
DM
DI
LIPv
LIPd
7a
DP
MST
V3
MT
V4
V4t
FST
STP
V1
V4
V2
V3
TVP
10 mm
A

FIGURE 9A.

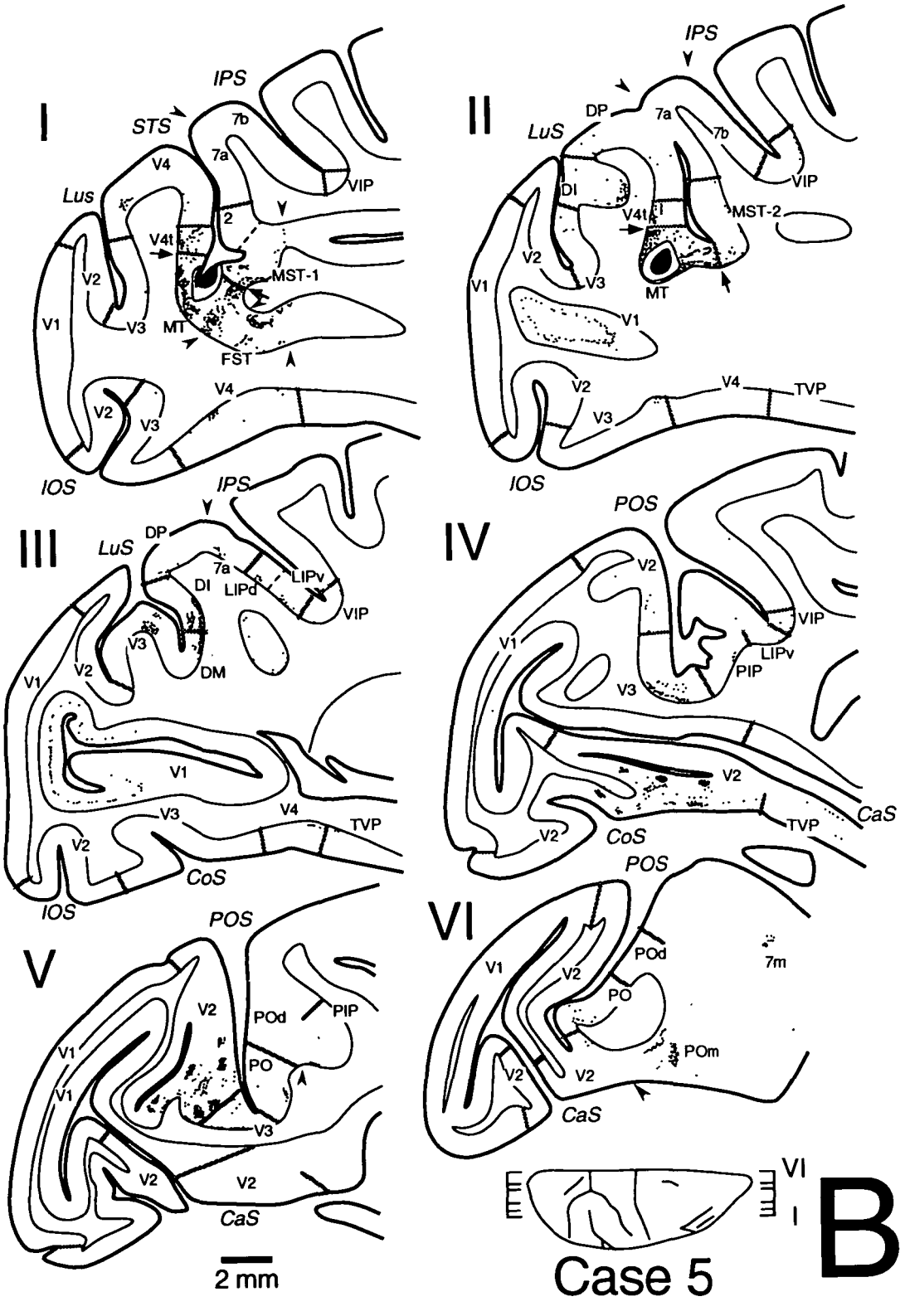

Fig. 9. Summary of data from case 5. Injection involved layers I to VI in MT, and layers I and II in MST. Conventions are as in Fig. 5.

In FST, no obvious topography was revealed by our data. However, some predominance of central representation may exist, as revealed by the more extensive label in case 1 (injection at the central representation, Fig. 5) than in the cases with injections in the representation of the periphery (Figs. 6-10). Nearly all labeled cells in FST were infragranular.

Only a very crude retinotopic pattern of connections was observed between MT and V4t. Note, for example, the displace-

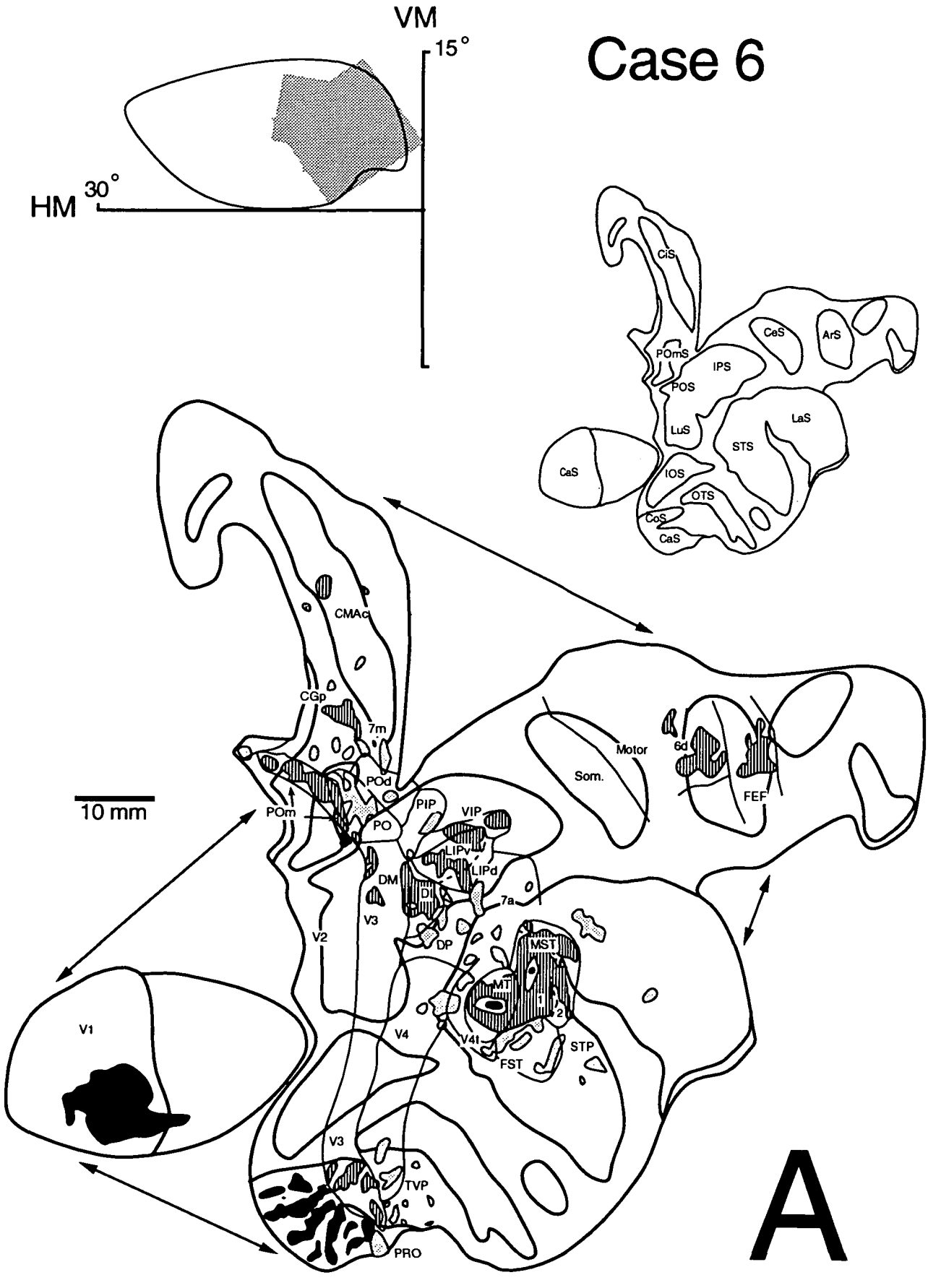
VM
15°
HM
30°
Case 6
CiS
CeS
ArS
POmS
IPS
POS
LaS
LuS
STS
CaS
IOS
OTS
CoS
CaS
CMAc
CGp
7m
POd
POm
PO
PIP
VIP
LIPv
LIPd
DM
DI
7a
V3
V2
DP
MST
MT
1
2
V4
V4t
STP
FST
V1
V3
TVP
PRO
Motor
Som.
6d
FEF
10 mm
A

FIGURE 10A.

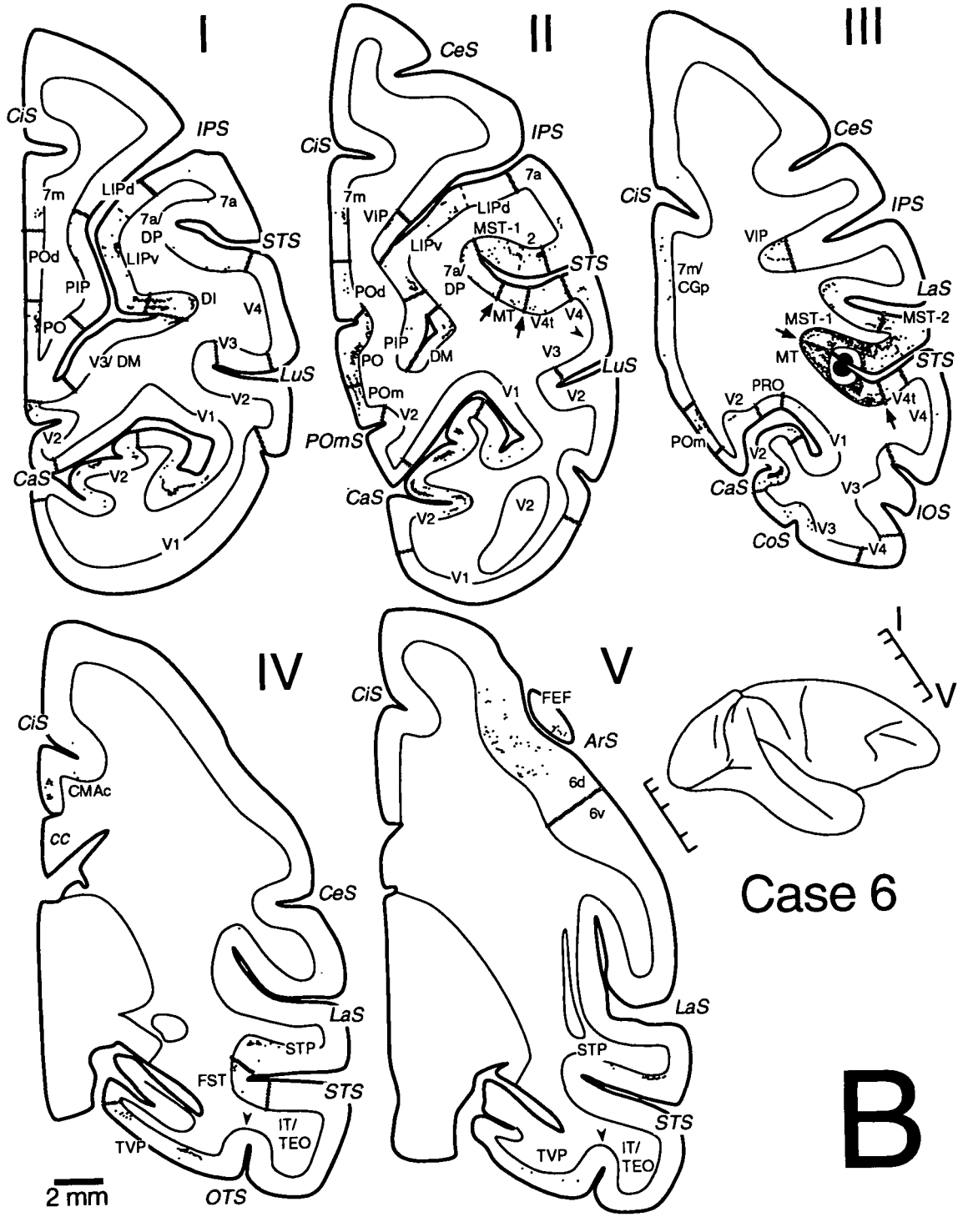

Fig. 10. Summary of data from case 6. Injection involved layers I to V in MT, and I to IV in MST. Conventions are as in Fig. 5. In this case, the brain was sectioned in an oblique plane equidistant from the coronal and the horizontal, as shown by the lateral reconstruction (insert at right).

ment of the heavily labeled patches towards the medial end of V4t in a case where the representation of the periphery was injected (e.g. Fig. 9) as compared with a case where the central representation was injected (Fig. 5). Unlike in the other STS areas described above, label in V4t was evenly distributed across supragranular and infragranular layers.

In two of the cases with injection restricted to MT (Figs. 5 and 8), as well as in both MT/MST cases, scattered infragranular labeled cells were also found anterior to MST and FST, in the dorsal bank of STS. These cells were assigned to the "superior temporal polysensory area" (STP; Bruce et al., 1981) on a regional basis only.

Intraparietal sulcus and POm

The main zone projecting to MT in the IPS was the heavily myelinated portion of area LIP (LIPv). However, the patches of label also spread to the less-myelinated neighboring cortex in the fundus and close to the lip of the sulcus (VIP and LIPd). Label in VIP and LIP seemed to be less extensive after an injection in the central representation (Fig. 5) than in the other cases. As in area MST, labeled cells in LIP formed a nearly continuous band in the infragranular layers, but some supragranular patches were also present. In VIP, however, only infragranular label was observed, with the exception of the cases with MST involvement. Occasional infragranular neurons were found a few millimeters lateral to the architectonic border of LIPd, but this may reflect the difficulty in defining a boundary in transition zones between architectonic patterns.

A complex of medially located areas showed projections to MT and/or MST in all but the case with the central injection (Fig. 5). In PIP, label appeared only in infragranular neurons irrespective of the invasion of MST by the injections. Patches in area PO consisted of continuous infragranular label and isolated supragranular cells. The projections from PO to MT were subject to topographic constraints. For example, an injection in the lower quadrant representation resulted in labeled cells only in the POS (Fig. 7), and an injection in the upper quadrant representation labeled only the precuneate gyrus (Fig. 10). In case 6, a patch with sparsely distributed infragranular neurons was found dorsal to PO, in the topographically appropriate portion of area POd. This was probably due to the MST involvement. Injections involving the HM representation labeled neurons in both sulcal and gyral PO (Figs. 6, 8, and 9).

In contrast, label in area POm had a marked supragranular component. The injections in cases 2 and 4, in the mid-peripheral HM representation in MT (Figs. 6 and 8), resulted in labeled patches both in the anterior, lower quadrant and in the posterior, upper quadrant representations of POm. In addition, an injection in the mid-peripheral lower quadrant representation (Fig. 7) resulted only in a small patch of label, in the anterior part of POm. However, the most extensive label in POm was seen after both injections involving MST (Figs. 9 and 10). In these cases, the supragranular component was as marked as the infragranular one, and label was widespread along virtually the whole extent of POm.

Areas TVP and prostriata

A crude visuotopy was present in the projections from TVP to MT. The injection in the central representation labeled cells in and around the OTS (Fig. 5), while the cases with injections in the mid-peripheral and peripheral representations labeled cells close to the lateral lip of the CaS. In addition, only isolated neurons were labeled after a lower quadrant injection (Fig. 7). Except for those in case 6 (Fig. 10), all labeled neurons in TVP were located in the infragranular layers. Also in case 6, a further patch of labeled neurons was observed in the area adjacent to TVP and anterior to V1 and V2 in the CaS. Based on its location and myeloarchitecture (Sanides, 1972; Gattass et al., 1987), we assigned this label to area prostriata.

Areas FEF and 6d

Whilst in the MT injection cases most of the label was located in patches around the anterior lip and anterior bank of the ArS, in the MT/MST cases considerable label was found in the posterior bank and posterior lip of the dorsal branch of the ArS, in area 6d. The position of the patches in FEF also varied according to the eccentricity of the injection, being more ventral in the case with injection in the central representation (Fig. 5) than in the cases with injections in the representations of the mid-periphery and periphery (e.g. Figs. 6 and 9).

Other areas labeled after injections involving MST

Both cases with MST involvement showed extensive infragranular label in DP and patches composed of scattered infragranular cells in 7a (Figs. 9 and 10). In these cases labeled cells were also present in an ensemble of areas located along the medial wall of the hemisphere. This is especially evident in Fig. 10, where the whole precuneate gyrus is labeled anterior to areas PO and POd. The label in this case involved much of area 7m of Cavada and Goldman-Rakic (1989), as well as more ventrally placed retrosplenial areas, probably including area CGp (Olson et al., 1992). A second focus of label in the medial wall was located more anteriorly, encompassing the ventral bank of the cingulate sulcus (CiS), in the approximate position of the caudal cingulate motor area (CMAc; Hutchins et al., 1988). This focus of label seems to correspond to an area that projects to the supplementary eye field (Huerta & Kaas, 1990).

Two different regions in the LaS also showed loosely packed patches of label after injections involving MST. One focus was located posteriorly, just in front of MST-2, along the fundus of the posterior tip of the LaS, and another overlaid the claustrum, at the ventral limit of the insular cortex. In both regions, labeled neurons were located only in infragranular layers.

Discussion

The regional pattern of connections of MT is similar in representatives of the two simian superfamilies, suggesting an homologous organization. By correlating the location of labeled neurons with architectonic subdivisions, we propose a model of the subdivisions of the visual cortex in a relatively large, diurnal and gyrencephalic New World monkey (Fig. 11). This illustration compiles data from many sources, and must be seen as a working hypothesis rather than a definitive model. This model has the merit of providing a coherent framework in which the connections of MT (present data) and V1 (Sousa et al., 1991) can be classified and interpreted in areal and retinotopic terms. Many of the same subdivisions can be recognized in previous models based on data from other genera. However, there are cases in which the subdivisions proposed here are not compatible with these models, and determining the exact number of homologous fields in the two simian lines will require a re-examination of the areal boundaries and, most desirably, a unification of the nomenclature. In our summary (Fig. 11), boundaries were placed only where there is independent evidence that a physiologically significant border is likely to occur at a given location, based either in studies of *Cebus* or in comparisons with other primates. Some of these boundaries are, however, provisional, and many uncertain points remain to be resolved by future studies. These controversial points, as well as likely homologies and comparisons with previous work, will be treated separately as they regard each area in the following sections.

Areas V1 and V2

Since MT is known to receive afferents from V1 in a range of primates (Kuypers et al., 1965; Spatz et al., 1970; Zeki, 1971*a*;

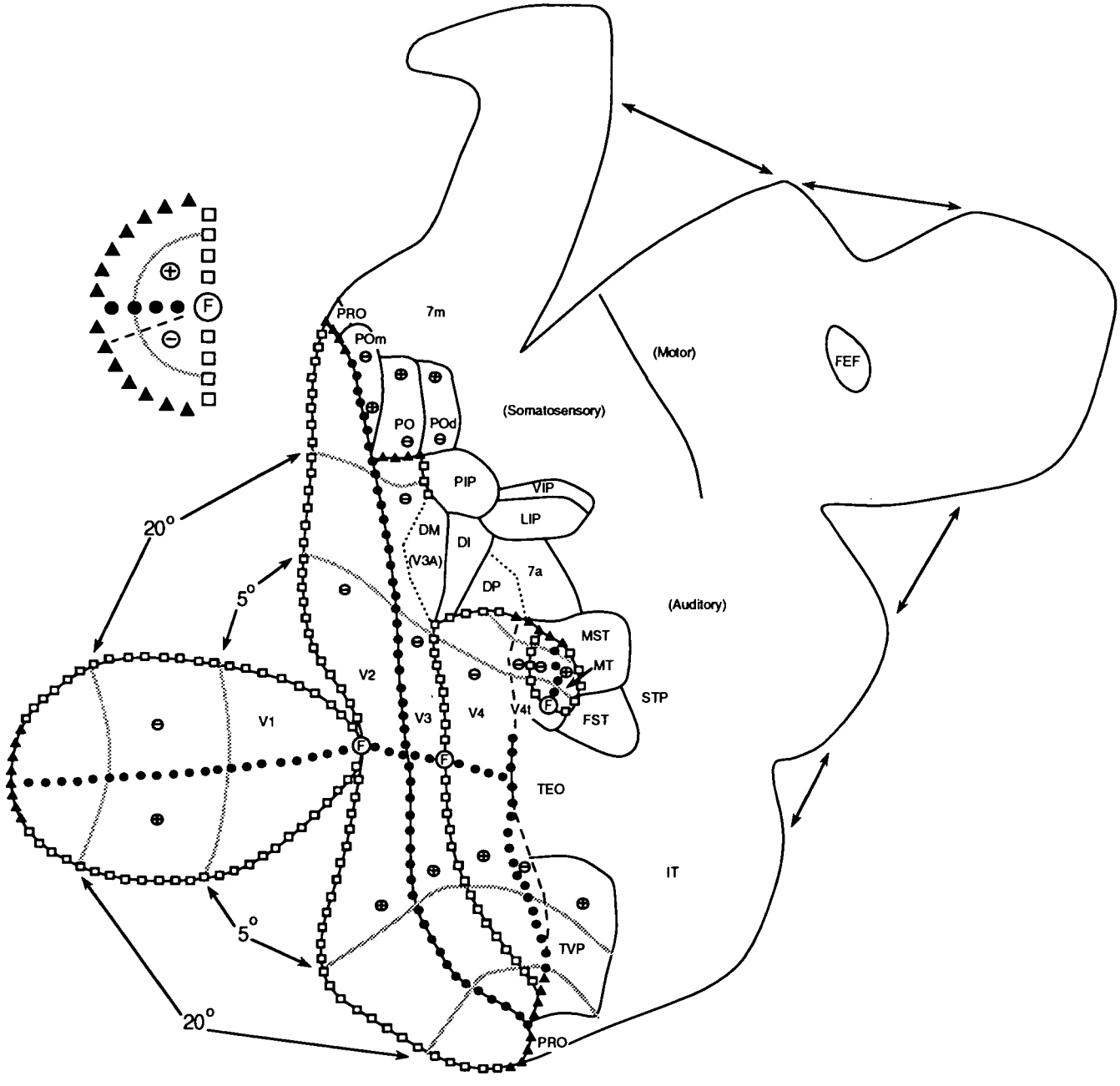

Fig. 11. Organization of visual cortex in *Cebus apella*, in a schematic flat map. For some areas, the visual topography is shown according to the insert (upper left): VM representations are indicated by squares, HM by dots, visual periphery by filled triangles, isoeccentricity lines by grey lines, an isopolar line in the lower quadrant by a dashed line, lower quadrant representations by the (−) sign, upper quadrant representations by the (+) sign, and the fovea by an (F). Dotted lines indicate borders that are not visible in myelin-stained sections. The visual topography and boundaries are based on the present data, complemented by the following other sources: V1 and PRO: Gattass et al. (1987); V2: Rosa et al. (1988); V3 and V4: Sousa et al., (1991); MT, MST, FST, and V4t: Fiorani et al. (1989); PO, POd, and POm: Neuenschwander (1989); and TVP: Sousa et al., (1991).

Spatz, 1977; Ungerleider & Mishkin, 1979), it is hardly surprising that we confirmed the existence of such connections in *Cebus*. As noted in previous studies (Spatz, 1977; Ungerleider & Desimone, 1986*b*; Krubitzer & Kaas, 1990), the estimate of the retinotopic extent of the injection sites based on the visual topography of V1 closely matched the receptive fields recorded at the injection sites. In addition, the laminar pattern of the MT-projecting neurons in V1 corresponds to that reported for other species (Spatz, 1977; Tigges et al., 1981; Maunsell & Van Essen, 1983*b*; Weller et al., 1984).

In area V2, we confirmed the existence of predominantly supragranular projections arranged in stripe-like patches. The center-to-center spacing between MT-projecting stripes roughly corresponds to the width of a cycle of cytochrome-oxidase stripes in *Cebus* (3–4 mm), an observation that supports previous proposals that only alternate cytochrome-oxidase-rich

stripes project to MT (De Yoe & Van Essen, 1985; Shipp & Zeki, 1985; Krubitzer & Kaas, 1990). Unpublished observations in our laboratory also demonstrate a correspondence between the MT-projecting stripes and Cat-301 rich patches in V2, as shown in the macaque (De Yoe et al., 1990).

Area V3

Present models of organization of extrastriate cortex in New World monkeys such as *Aotus* and *Saimiri* do not recognize an area comparable to V3 of the macaque. Instead, studies in these species suggest that multiple areas occupy the corresponding cortex anterior to V2 (Sereno & Allman, 1990; Kaas & Krubitzer, 1991; Weller et al., 1991). It has been proposed that the more dorsal portion of the macaque's V3 corresponds to part or all of area DM of New World monkeys (Lin et al., 1982; Burkhalter et al., 1986; Krubitzer & Kaas, 1990; Sereno & Allman, 1990; Kaas & Krubitzer, 1991; Weller et al., 1991), based on its location, myeloarchitecture, and on the fact that DM receives projections from V1. In addition, the ventral part of V3 would be homologous to the ventral posterior area (VP), as suggested by Newsome et al. (1986). However, most authors have been cautious in proposing an exact correspondence between dorsal V3 and DM. Although DM represents (at least in the owl monkey) the whole contralateral hemifield, dorsal V3 represents only the lower quadrant. Moreover, in the *Cebus* the whole extrastriate belt anterior to V2 projects back to V1 (Sousa et al., 1991), and the differences in myelination between dorsal and ventral V3 are inconsistent (in agreement with observations by Ungerleider & Desimone, 1986*b*, in the macaque). Therefore, the anatomical asymmetry between dorsal and ventral V3 is not marked. Finally, a heavier myelination in the lower quadrant representation could merely reflect different specializations of lower *vs.* upper quadrants (Previc, 1990). For example, the use of a strict myeloarchitectonic criterion in the delimitation of the macaque's area MT reveals a strong bias towards lower quadrant representation (Maunsell & Van Essen, 1987) that is not as marked if anatomical and physiological criteria are also considered (Desimone & Ungerleider, 1986).

These arguments call attention to other possibilities. For example, the anterior limit of dorsal V3 with area V3A in the macaque is hard to define in myeloarchitectonic terms (Gattass et al., 1988*a*). Both dorsal V3 and V3A are known to receive projections from V1 (Zeki, 1980), but only V3A represents both quadrants of the contralateral hemifield (Van Essen & Zeki, 1978; Gattass et al., 1988*a*). Thus, it is likely that the densely myelinated subdivision anterior to V2 includes two areas, namely a portion of V3 proper, posteriorly, and DM (or "V3A"), anteriorly. This hypothesis would explain the less-clear visual topography in the extrastriate belt immediately anterior to dorsal V2, as compared with that anterior to ventral V2, in the data here reported. Based on the current evidence, we consider this the most likely hypothesis on the organization of the extrastriate belt anterior to V2. Another possibility is that the area homologous to DM is not V3 or V3A, but area PO. This area stains darker for myelin than any other dorsal area, including V3, and therefore would correspond to the definition of DM proposed by Krubitzer and Kaas (1990). Area PO also receives projections from V1 (Colby et al., 1988) and represents both quadrants, although with the upper quadrant lying medially rather than laterally as in the owl monkey's DM. Although the tendency in the literature is to consider PO as homologous with the owl monkey's medial area (M; Allman & Kaas, 1976; Gattass et al., 1985; Colby et al., 1988), the evidence for other medially located visual areas with emphasis on peripheral representation (POd and POm; Neuenschwander, 1989; Gattass et al., 1990) raises the possibility that one of these areas may correspond to M, while PO corresponds to DM. Alternatively, the architectonic area DM of Krubitzer and Kaas (1990) could encompass part of V3 and area PO, areas V3A and PO, or all of these together.

Connections of the extrastriate belt immediately anterior to V2 with MT can be observed in all of the previously published studies on MT connections. These connections were variously attributed to "foci 7 and 8" (Spatz & Tigges, 1972), "area 19" (Tigges et al., 1981), "areas V3 and VP" (Maunsell & Van Essen, 1983*b*), "DM/caudal DL/ventral visual area" (Weller et al., 1984; Steele et al., 1991), and "cortex around the inferotemporal sulcus" (Krubitzer & Kaas, 1990). In addition, Ungerleider and Desimone (1986*b*) referred to the strip of cortex anterior to V2 as "V3," as we do. Interestingly, all of the studies employing retrograde tracer injections in MT agree on the fact that projections from this region arise mainly from layer III, therefore conforming to the laminar characteristic of "feedforward connections." In contrast, in our study projections from V3 to MT were characterized by patches containing infragranular and supragranular neurons in roughly the same number intermixed with patches with clear infragranular predominance.

Areas V4 and V4t

Area V4, a name coined by Zeki (1971*b*) to define a target zone of V2 projections in and around the prelunate gyrus of the macaque, was later mapped in detail by Gattass et al. (1985, 1988*a*). The *Cebus* monkey's area V4 resembles the macaque's V4 in its extent and position relative to other areas, has similar myeloarchitectonic characteristics, and projects with a clear topographic order and a well-defined laminar pattern to both V1 and MT (Sousa et al., 1991). It has been suggested that V4 is homologous to the dorsolateral area (DL) of New World monkeys (Allman & Kaas, 1974; Weller & Kaas, 1985; Kaas & Krubitzer, 1991; Steele et al., 1991), in view of single-unit properties (Baker et al., 1981; Desimone & Schein, 1987), location, a large representation of foveal vision, and connections with inferotemporal cortex (Desimone et al., 1980; Weller & Kaas, 1985). In recent years, however, area DL has been subdivided into two areas along the antero-posterior dimension (Cusick & Kaas, 1988; Sereno et al., 1987; Sereno & Allman, 1990), and a third area immediately adjacent to MT has been described (DLa of Sereno & Allman, 1990; "MT crescent" of Kaas & Morel, 1993) (see Fig. 1). If *Cebus* is compared with Sereno and Allman's (1990) model of owl monkey visual areas (Fig. 1B), the most likely homologies are between V3 and areas DLp/VP, V4 and DLi/VA, and V4t and area DLa. One would expect, based on preliminary reports (Newsome & Allman, 1980; Sereno et al., 1987), to find mainly upper quadrant representation in VP and VA, lower quadrant representation in DLp and DLi, and a representation of the VM separating DLp/VP from DLi/VA. This configuration would suggest a single area adjoining V2, similar to V3, bounded anteriorly by another area homologous to V4. Comparisons with DLc and DLr (caudal and rostral subdivisions of area DL) defined in *Saimiri* and *Aotus* (Steele et al., 1991; Fig. 1A) are less clear, in view of the different methods and criteria used to define these regions. DLc is usually depicted as much wider than DLr, and both areas are largely restricted to the lateral surface of the occipital lobe. They may correspond to the central representation in V3 and V4, a

hypothesis that would explain the heavy connections between DL and IT cortex (Weller & Kaas, 1985; Ungerleider et al., 1986; Steele et al., 1991).

Projections from V4 (or "DL") to MT were observed in previous studies (Maunsell & Van Essen, 1983*b*; Weller et al., 1984; Ungerleider & Desimone, 1986*b*; Krubitzer & Kaas, 1990; Steele et al., 1991). In contrast to previous reports, however, in *Cebus* virtually all labeled cells in V4 after MT injections are infragranular. As previously indicated by studies in both Platyrrhine (Krubitzer & Kaas, 1990; Sousa et al., 1991; Steele et al., 1991) and Catarrhine (Gattass et al., 1988*a*) monkeys, our data demonstrates the great emphasis on central representation in V4. This is compatible with its assignment to the "ventral stream" of extrastriate areas likely to process attributes of an image such as shape, texture, and color (Desimone et al., 1980; Ungerleider & Mishkin, 1982; Weller & Kaas, 1985; Gattass et al., 1990; Krubitzer & Kaas, 1990; Boussaoud et al., 1991).

Areas MST, FST, STP, and lateral sulcus

We confirm the basic finding of previous reports (Spatz & Tigges, 1972; Wall et al., 1982; Maunsell & Van Essen, 1983*b*; Weller et al., 1984; Ungerleider & Desimone, 1986*b*; Krubitzer & Kaas, 1990) that many of the connections of MT relate to immediately adjoining areas. Our results also support the existence of an emphasis on central representation in FST, and a large peripheral representation in MST (Weller et al., 1984; Fiorani et al., 1989; Boussaoud et al., 1990). Although studies in the macaque (Desimone & Ungerleider, 1986; Boussaoud et al., 1990) usually regard the anterior border of the densely myelinated zone of the anterior bank of STS as the outer limit of MST, in *Cebus* we found cells projecting to MT a few millimeters beyond this boundary. However, these neurons were not as densely packed as those found in heavily myelinated MST (MST-1), and, with rare exceptions, were found only in infragranular layers. Some cases also showed sparse label in areas located even more anteriorly in the STS and LaS. Similar connections have been previously noted in studies of MST projections in *Aotus* (Weller et al., 1984) and MT connections in *Galago* (Krubitzer & Kaas, 1990). Studies in the macaque were unable to find evidence of projections of the LaS areas to MT and MST (Ungerleider & Desimone, 1986*b*; Boussaoud et al., 1990). However, in macaques the LaS projects to the lateral bank of the IPS, which is strongly connected with both MT and MST (Cavada & Goldman-Rakic, 1989; Blatt et al., 1990). Thus, there is an oligosynaptic pathway between MT and polysensory cortex in the anterior bank of STS and in the LaS.

Areas VIP and LIP

Area VIP was defined by Maunsell and Van Essen (1983*b*) as the target of MT projections in the IPS. However, more recent evidence from physiological recordings in the macaque demonstrated two areas in this region (Andersen et al., 1990; Colby et al., 1993). The properties of neurons in the lateral bank of IPS point to a clear separation between LIP and VIP (Colby et al., 1993), and provide a good example of the point that single areas may vary in their architectonic aspect (Andersen et al., 1990). Perhaps the most significant result regarding these areas, in our study, is the remarkable similarity in location and architectonic characteristics of VIP and LIP in *Cebus* and *Macaca*. A densely myelinated field in the ventral posterior parietal cortex has also been observed in the owl monkey (Kaas & Krubitzer, 1991) that may correspond to LIPv. Thus, LIP and VIP are likely to be among visual areas that are common to all simians, and may have first appeared at least 30 million years ago, before the Platyrrhine/Catarrhine dichotomy (Fleagle, 1988).

It is clear from studies in different primates that the ventral parietal cortex is an important source of projections to MT (Maunsell & Van Essen, 1983*b*; Weller et al., 1984; Ungerleider & Desimone, 1986*b*; Krubitzer & Kaas, 1990). Area LIP, like MST and FST, is one of the main targets of "feedforward" connections from MT. However, unlike MST and FST, LIP has restricted receptive fields and a relatively clear visual topography (Blatt et al., 1990). The fact that retinotopic order is preserved in LIP and the presence of presaccadic and especially "saccadic memory" neurons in this area (Andersen & Gnadt, 1989) suggest that the IPS visual areas may be related to saccadic preparation and visuomotor orientation to specific portions of the visual space. In contrast, MST may be more involved in flow-field processing, optokinetic eye movement programming, and other aspects of visuomotor coordination that require the analysis of global rather than local features (Duffy & Wurtz, 1991). The more extensive connections of FST with the anterior STS, including parts of the inferotemporal cortex (Boussaoud et al., 1990; Morel & Bullier, 1990), suggest a participation in the integration of motion and form information for pattern recognition and figure-ground segregation (Baylis et al., 1987; Boussaoud et al., 1990).

Area DI

This region was included as part of a more extensive "annectent region" in a previous study of *Cebus* (Sousa et al., 1991), and was found to project very sparsely to lower quadrant V1. The present data enabled us to define the anterior boundary of DI by using the presence of connections with MT and MST as criteria. Although its location anterior to V3 could suggest an homology with the macaque's area V3A (Van Essen & Zeki, 1978; Gattass et al., 1988*a*), there are reasons why a homology between DI and V3A is unlikely. In contrast with V3A, DI is readily separable from V3 in myeloarchitectonic terms. Moreover, while both dorsal V3 and V3A in the macaque are rich in Cat-301-positive neurons (De Yoe et al., 1990), DI is not (unpublished results). In comparison with other New World monkeys, the ill-defined visuotopy, architectonic characteristics, location, and projections to MT suggest that this region may correspond to the myeloarchitectonic area DI as redefined by Krubitzer and Kaas (1990). Connections of MT and DI were also observed in the owl monkey by Weller et al. (1984), and part of the label attributed to "V3A" by Ungerleider and Desimone (1986*b*) may also belong to a homologous region in the macaque. Projections from DI to MT are reported to arise mainly from supragranular layers, and in this respect the laminar distribution we observed in DI of *Cebus* is unusual.

Medial extrastriate cortex and arcuate sulcus

The extensive label in PO and POm after injections involving peripheral MT and/or MST provide further evidence for the existence of a complex of medially located areas which emphasize the representation of the visual-field periphery. Although some of the visual motion areas in STS, including MT and central MST, seem to send projections mainly to the lateral intraparietal subdivision of the posterior parietal cortex (PP), area PO and peripheral MST are also connected to the inferior parietal gyrus (area 7a) and to portions of PP cortex in the dorsal tip of the anterior bank of STS (Colby et al., 1988; Boussaoud

et al., 1990). These two parallel circuits, emphasizing central and peripheral motion processing, respectively, may reflect the psychophysical evidence for two parallel motion analysis systems dealing differently with central and peripheral space (Dichgans & Brandt, 1974; Gattass et al., 1990). Evidence for the connections between MT and PO is present in studies of other species (Weller et al., 1984; Ungerleider & Desimone, 1986*b*; Colby et al., 1988). Since the evidence for other subdivisions in the PO complex is recent, one cannot be sure of the existence of the connections between POm and MT/MST in other primates. An examination of the cases reported by Weller et al. (1984) and Boussaoud et al. (1990) suggests that some of the label attributed to V2 and PO (or medial visual area, M) may in fact belong to POm. Another region apparently devoted to peripheral vision is PIP. Apart from a report of projections to PO (Colby et al., 1988), little is known about this area. It is likely that the region we defined as PIP encompasses both the macaque's areas PIP and medial intraparietal (MIP; Colby et al., 1988), but this point will remain unresolved until future work combining myeloarchitecture with electrophysiology and connections in this region.

Besides confirming the existence of sparse connections between MST and area 7a, our results demonstrate projections from the medial subdivision of the PP cortex (area 7m), from caudal cingulate cortex and from the posterior bank of the ArS to MST. Connections of MST with the region anterior to areas M and PO were observed by Weller et al. (1984) in the owl monkey and by Cavada and Goldman-Rakic (1989) in the macaque. The anteromedial extrastriate region in the macaque has also been reported to project to area PO (Colby et al., 1988), and some of the label observed in medial extrastriate cortex by Boussaoud et al. (1990; e.g. their Fig. 3) is also likely to belong to 7m. In addition, cortex corresponding to one of the MST-projecting medial areas in *Cebus* was recently found to be visually responsive, and is believed to be involved in visuomotor and visuospatial functions in the macaque (Olson et al., 1992).

Although no connections between MST and area 6d were reported in a recent study in the macaque (Boussaoud et al., 1990), in this genus the homologous region seems to project to another "dorsal stream" area, PO (see Fig. 8H in Colby et al., 1988). The MST-projecting subdivision of the premotor area may be involved in oculomotor behavior (Bon & Lucchetti, 1990).

Area TVP

The findings of this report confirm the conclusions of Sousa et al. (1991) regarding the extent and topographic organization of visual area TVP. Studies in the macaque suggest the existence of either a single, strip-like area (Felleman & Van Essen, 1991) or two areas (Boussaoud et al., 1991) bordering ventral V4 anteriorly. Our results favor the second hypothesis. While TVP projects to both MT and V1 (present results; Sousa et al., 1991), the area located lateral to the OTS does not. We refer to the latter as TEO by analogy with the macaque (Boussaoud et al., 1991). In *Cebus*, however, the border between the two areas is located lateral, instead of medial, to the OTS, and TVP seems to have an enlarged central representation (Sousa et al., 1991). Connections of TVP with MT have not been previously reported, but this may only reflect a less-complete definition of areal boundaries in previous work. For example, some of the squirrel monkey and marmoset MT injection cases illustrated by Krubitzer and Kaas (1990) provide particularly striking examples of retrograde label in the TVP region (e.g. their Fig. 20).

Laminar distribution and functional hierarchies

The concept of "feedforward" and "feedback" patterns of connections among visual areas was initially derived from observations on the anterogradely mapped connections between V1 and V2 (Kuypers et al., 1965; Tigges et al., 1973). The basic concept was shown to be valid in other portions of the visual cortex as well, and was expanded to include results based on retrograde tracers (Lund et al., 1975; Wong-Riley, 1978; Rockland & Pandya, 1979; Tigges et al., 1981; Maunsell & Van Essen, 1983*b*; Andersen et al., 1990). These studies indicate that "forward" connections arise predominantly from cells in the supragranular layers of a given area and terminate predominantly in layer IV. In contrast, "backward" connections arise mainly from infragranular layers of a given area and their termination sites avoid layer IV. Based on these principles, Maunsell and Van Essen (1983*b*) arranged extrastriate areas in hierarchical levels, and the same concept has also been used to fit other areas in hierarchical levels (Colby et al., 1988; Boussaoud et al., 1990; Andersen et al., 1990; Felleman & Van Essen, 1991). Maunsell and Van Essen (1983*b*) have further recognized the existence of "intermediate" patterns of connections, and hypothesized that these would constitute links between areas at similar hierarchical levels.

Application of these criteria to our data (Fig. 12) suggests that in the *Cebus* (1) only areas V1 and V2 would send "feedforward" projections to MT; (2) areas V3, DM, POm, V4t, and perhaps DI would be at the same hierarchical level; and (3) all of the other areas, including V4 and PO, would send "backwards" projections to MT. This scheme is different from those proposed for the macaque, in which MT and V4t are moved one step further in the hierarchy to lie at the same level as V4 and PO (Maunsell & Van Essen, 1983*b*; Colby et al., 1988; Boussaoud et al., 1990). In addition, results of studies in other New World monkeys suggest that they are likely to resemble the macaque rather than *Cebus* since a relatively large number of

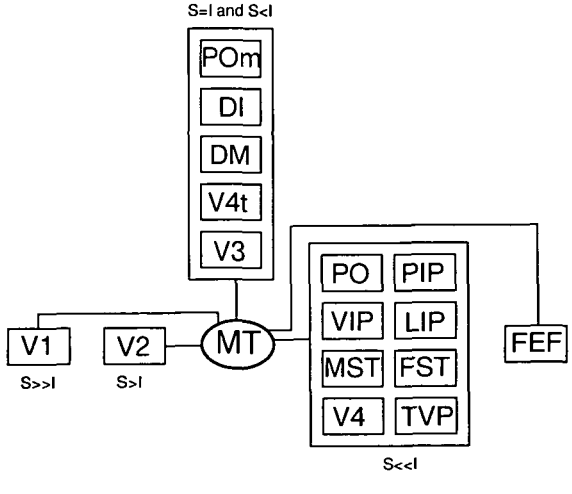

Fig. 12. Projections to area MT in *Cebus*, according to laminar patterns. S ≫ I—almost exclusively supragranular projection; S > I—supragranular predominance; S = I—supragranular and infragranular cells in roughly the same numbers; S < I—infragranular predominance; and S ≪ I—almost exclusively infragranular projection. The projection from the FEF to MT was variable in its laminar involvement, but usually included infragranular as well as supragranular cells.

supragranular MT-projecting cells is observed in areas DM, DI, DL, and VP (Weller et al., 1984; Krubitzer & Kaas, 1990). These differences are unlikely to reflect tracer sensitivities (e.g. Fast Blue *vs.* HRP), since we in fact observe *less* laminar involvement than previous studies. Moreover, Sousa et al. (1991), using fluorescent tracers, also observed that the "backward" prestriate projections to V1 in *Cebus* show a much more marked infragranular emphasis than that reported in a similar study in the macaque (Perkel et al., 1986). Thus, laminar patterns, and specifically the relative numbers of projecting cells in the infragranular and supragranular layers, are labile characters in evolutionary terms. Whether this indicates that the hierarchical position of a given area may also vary across species, or that the patterns revealed by retrograde tracers are not reliable in establishing hierarchies (as suggested by Felleman & Van Essen, 1991), will require further work.

Acknowledgments

The authors would like to thank Dr. Aglai P.B. Sousa for her invaluable help throughout this work; Dr. Leah Krubitzer, Dr. Maree J. Webster, Dr. David Pow, Ms. Rowan Tweedale, and Ms. Leisa Schmid for many suggestions on the preparation of the manuscript; Edil S. Silva Filho for the histology; and Danny Thomas for help with the computers. Cat-301 antibody was supplied by Susan Hockfield, from Yale University. This research was supported by grants from FINEP, CNPq, and FAPERJ (Brazil) and ARC (Australia).

References

Allman, J.M. & Kaas, J.H. (1971). A representation of the visual field in the caudal third of the middle temporal gyrus of owl monkeys (*Aotus trivirgatus*). *Brain Research* **31**, 85–105.

Allman, J.M. & Kaas, J.H. (1974). A crescent-shaped cortical visual area surrounding the middle temporal area (MT) in the owl monkey (*Aotus trivirgatus*). *Brain Research* **81**, 199–213.

Allman, J.M. & Kaas, J.H. (1975). The dorsomedial cortical visual area: A third tier area in the occipital lobe of the owl monkey. (*Aotus trivirgatus*). *Brain Research* **100**, 473–487.

Allman, J.M. & Kaas, J.H. (1976). Representation of the visual field in the medial wall of the occipital-parietal cortex in the owl monkey. *Science* **191**, 572–576.

Allman, J.M., Kaas, J.H. & Lane, R.H. (1973). The middle temporal visual area (MT) in the bushbaby (*Galago senegalensis*). *Brain Research* **57**, 197–202.

Andersen, R.A., Asanuma, C., Essick, G. & Siegel, R.M. (1990). Corticocortical connections of anatomically and physiologically defined subdivisions within the inferior parietal lobule. *Journal of Comparative Neurology* **296**, 65–113.

Andersen, R.A. & Gnadt, J.W. (1989). Role of posterior parietal cortex in saccadic eye movements. In *Reviews in Oculomotor Research, Vol. 3*, ed. Wurtz, R. & Goldberg, M., pp. 315–335. Amsterdam: Elsevier.

Baker, J.F., Petersen, S.E., Newsome, W.T. & Allman, J.M. (1981). Visual response properties of neurons in four extrastriate visual areas of the owl monkey (*Aotus trivirgatus*): A quantitative comparison of medial, dorsomedial, dorsolateral, and middle temporal areas. *Journal of Neurophysiology* **45**, 397–416.

Baylis, G.C., Rolls, E.T. & Leonard, C.M. (1987). Functional subdivisions of temporal lobe neocortex. *Journal of Neuroscience* **7**, 330–342.

Blatt, G.J., Andersen, R.A. & Stoner, G.R. (1990). Visual receptive-field organization and cortico-cortical connections of the lateral intraparietal area (Area LIP) in the macaque. *Journal of Comparative Neurology* **299**, 421–445.

Bon, L. & Lucchetti, C. (1990). Neurons signalling the maintenance of attentive fixation in frontal area 6aβ of macaque monkey. *Experimental Brain Research* **82**, 231–233.

Boussaoud, D., Desimone, R. & Ungerleider, L.G. (1991). Visual topography of area TEO in the macaque. *Journal of Comparative Neurology* **306**, 554–575.

Boussaoud, D., Ungerleider, L.G. & Desimone, R. (1990). Pathways for motion analysis: Cortical connections of the medial superior temporal and fundus of the superior temporal visual areas in the macaque. *Journal of Comparative Neurology* **296**, 462–495.

Bruce, C.J., Desimone, R. & Gross, C.G. (1981). Properties of neurons in a visual polysensory area in the superior temporal sulcus of the macaque. *Journal of Neurophysiology* **46**, 369–384.

Bruce, C.J., Goldberg, M.E., Bushnell, M.C. & Stanton, G.B. (1985). Primate frontal eye fields. II. Physiological and anatomical correlates of electrically evoked eye movements. *Journal of Neurophysiology* **54**, 714–734.

Burkhalter, A., Felleman, D.J., Newsome, W.T. & Van Essen, D.C. (1986). Anatomical and physiological asymmetries related to visual areas V3 and VP in macaque extrastriate cortex. *Vision Research* **26**, 63–80.

Cavada, C. & Goldman-Rakic, P.S. (1989). Posterior parietal cortex in rhesus monkey. I: Parcelation of areas based on distinctive limbic and sensory cortico-cortical connections. *Journal of Comparative Neurology* **287**, 393–421.

Colby, C.L., Gattass, R., Olson, C.R. & Gross, C.G. (1988). Topographical organization of cortical afferents to extrastriate area PO in the macaque: A dual tracer study. *Journal of Comparative Neurology* **269**, 392–413.

Colby, C.L., Duhamel, J.N. & Goldberg, M.E. (1993). The ventral intraparietal area (VIP) of the macaque: Anatomical location and visual response properties. *Journal of Neurophysiology* **69**, 902–914.

Conde, F. (1987). Further studies on the use of the fluorescent tracers Fast blue and Diamidino yellow: Effective uptake area and cellular storage sites. *Journal of Neuroscience Methods* **21**, 31–43.

Cusick, C.G. & Kaas J.H. (1988). Cortical connections of area 18 and dorsolateral visual cortex in squirrel monkeys. *Visual Neuroscience* **1**, 211–237.

Desimone, R., Fleming, J. & Gross, C.G. (1980). Prestriate afferents to inferior temporal cortex: An HRP study. *Brain Research* **184**, 41–55.

Desimone, R. & Schein, S.J. (1987). Visual properties of neurons in area V4 of the macaque: Sensitivity to stimulus form. *Journal of Neurophysiology* **57**, 835–867.

Desimone, R. & Ungerleider, L.G. (1986). Multiple visual areas in the caudal superior temporal sulcus of the macaque. *Journal of Comparative Neurology* **248**, 164–189.

De Yoe, E.A., Hockfield, S., Garren, H. & Van Essen, D.C. (1990). Antibody labeling of functional subdivisions in visual cortex: Cat-301 immunoreactivity in striate and extrastriate cortex of the macaque monkey. *Visual Neuroscience* **5**, 67–81.

De Yoe, E.A. & Van Essen, D.C. (1985). Segregation of efferent connections and receptive-field properties in visual area V2 of the macaque. *Nature* **317**, 58–61.

Dichgans, J. & Brandt, T.H. (1974). The psychophysics of visually induced perception of self-motion and tilt. In *The Neurosciences—Third Study Program, Vol. III*, ed. Schmitt, F.O. & Worden, F.G., pp. 123–129. Cambridge: MIT Press.

Duffy, C.J. & Wurtz, R.H. (1991). Sensitivity of MST neurons to optic flow stimuli: I. A continuum of response selectivity to large-field stimuli. *Journal of Neurophysiology* **65**, 1329–1345.

Felleman, D.J. & Kaas, J.H. (1984). Receptive-field properties of neurons in the middle temporal visual area (MT) of owl monkeys. *Journal of Neurophysiology* **52**, 488–513.

Felleman, D.J. & Van Essen, D.C. (1991). Distributed hierarchical processing in primate cerebral cortex. *Cerebral Cortex* **1**, 1–47.

Fiorani, M., Jr., Gattass, R., Rosa, M.G.P. & Sousa, A.P.B. (1989). Visual area MT in the *Cebus* monkey: Location, visuotopic organization, and variability. *Journal of Comparative Neurology* **287**, 98–118.

Fleagle, J.G. (1988). *Primate Adaptation and Evolution*. San Diego, California: Academic Press.

Gallyas, F. (1979). Silver staining of myelin by means of physical development. *Neurology Research* **1**, 203–209.

Gattass, R. & Gross, C.G. (1981). Visual topography of the striate projection zone in the posterior superior temporal sulcus (MT) of the macaque. *Journal of Neurophysiology* **46**, 521–538.

Gattass, R., Rosa, M.G.P., Sousa, A.P.B., Piñon, M.C., Fiorani, M., Jr. & Neuenschwander, S. (1990). Cortical streams of visual

information processing in primates. *Brazilian Journal of Medical and Biological Research* **23**, 375–393.

GATTASS, R., SOUSA, A.P.B. & COVEY, E. (1985). Cortical visual areas of the macaque: Possible substrates for pattern recognition mechanisms. In *Pattern Recognition Mechanisms*, ed. CHAGAS, C., GATTASS, R. & GROSS, C.G., pp. 1–20. Vatican City: Pontificial Academy of Sciences.

GATTASS, R., SOUSA, A.P.B. & ROSA, M.G.P. (1987). Visual topography of V1 in the *Cebus* monkey. *Journal of Comparative Neurology* **259**, 529–548.

GATTASS, R., SOUSA, A.P.B. & GROSS, C.G. (1988*a*). Visuotopic organization and extent of V3 and V4 of the macaque. *Journal of Neuroscience* **8**, 1831–1845.

GATTASS, R., SOUSA, A.P.B., ROSA, M.G.P. & PIÑON, M.C. (1988*b*). Ventral V3 in the *Cebus* monkey: Visual topography and projections to V1. *Society for Neuroscience Abstracts* **14**, 202.

HOCKFIELD, S., MCKAY, R.D.G., HENDRY, S.H.C. & JONES, E.G. (1983). A surface antigen that identifies ocular-dominance columns in the visual cortex and laminar features of the lateral geniculate nucleus. *Cold Spring Harbor Symposium on Quantitative Biology* **48**, 877–889.

HUERTA, M.F. & KAAS, J.H. (1990). Supplementary eye field as defined by intracortical microstimulation: Connections in macaques. *Journal of Comparative Neurology* **293**, 299–330.

HUTCHINS, K.D., MARTINO, A.M. & STRICK, P.L. (1988). Corticospinal projections from the medial wall of the hemisphere. *Experimental Brain Research* **71**, 667–672.

KAAS, J.H. & KRUBITZER, L.A. (1991). The organization of extrastriate visual cortex. In *Neuroanatomy of the Visual Pathways and Their Development*, ed. DREHER, B. & ROBINSON, S.R., pp. 302–323. London: Macmillan.

KAAS, J.H. & MOREL, A. (1993). Connections of visual areas of the upper temporal lobe of owl monkeys: The MT crescent and dorsal and ventral subdivisions of FST. *Journal of Neuroscience* **13**, 534–546.

KRUBITZER, L.A. & KAAS, J.H. (1990). Cortical connections of MT in four species of primates: Areal, modular, and retinotopic patterns. *Visual Neuroscience* **5**, 165–204.

KUYPERS, H.G.J.M., SZWARCBART, M.K., MISHKIN, M. & ROSVOLD, H.E. (1965). Occipitotemporal corticocortical connections in the rhesus monkey. *Experimental Neurology* **11**, 245–262.

LE GROS CLARK, W.E. (1959). *The Antecedents of Man*. Edinburgh: University Press.

LENNIE, P., KRAUSKOPF, J. & SCLAR, G. (1990). Chromatic mechanisms in striate cortex of macaque. *Journal of Neuroscience* **10**, 649–669.

LIN, C.S., WELLER, R.E. & KAAS, J.H. (1982). Cortical connections of striate cortex in owl monkeys. *Journal of Comparative Neurology* **211**, 165–176.

LUND, J.S., LUND, R.D., HENDRICKSON, A.E., BUNT, A.H. & FUCHS, A.F. (1975). The origin of efferent pathways from the primary visual cortex, area 17, of the macaque monkey as shown by retrograde transport of horseradish peroxidase. *Journal of Comparative Neurology* **164**, 287–304.

MAUNSELL, J.H.R. & VAN ESSEN, D.C. (1983*a*). Functional properties of neurons in the middle temporal visual area of the macaque monkey. I. Selectivity for stimulus direction, speed, and orientation. *Journal of Neurophysiology* **49**, 1127–1147.

MAUNSELL, J.H.R. & VAN ESSEN, D.C. (1983*b*). The connections of the middle temporal visual area (MT) and their relationship to a cortical hierarchy in the macaque monkey. *Journal of Neuroscience* **3**, 2563–2586.

MAUNSELL, J.H.R. & VAN ESSEN, D.C. (1987). Topographic organization of the middle temporal visual area in the macaque monkey: Representational biases and the relationship to callosal connections and myeloarchitectonic boundaries. *Journal of Comparative Neurology* **266**, 535–555.

MOREL, A. & BULLIER, J. (1990). Anatomical segregation of two cortical visual pathways in the macaque monkey. *Visual Neuroscience* **4**, 555–578.

NEUENSCHWANDER, S. (1989). *Área visual parieto-occipital do Cebus apella: Um estudo anatômico e eletrofisiológico*. MSc. Thesis, Rio de Janeiro, Universidade Federal do Rio de Janeiro.

NEWSOME, W.T. & ALLMAN, J.M. (1980). Interhemispheric connections of visual cortex in the owl monkey *Aotus trivirgatus* and the bushbaby *Galago senegalensis*. *Journal of Comparative Neurology* **194**, 209–233.

NEWSOME, W.T., MAUNSELL, J.H.R. & VAN ESSEN, D.C. (1986). Ventral posterior visual area of the macaque: Visual topography and areal boundaries. *Journal of Comparative Neurology* **252**, 139–153.

OLSON, C.R., MUSIL, S.Y. & GOLDBERG, M.E. (1992). Posterior cingulate cortex and visuospatial cognition: Properties of neurons in the behaving monkey. In *The Neurobiology of Cingulate Cortex and Limbic Thalamus*, ed. VOGT, B.A. & GABRIEL, M. Boston: Birkhauser (in press).

PERKEL, D.J., BULLIER, J. & KENNEDY, H. (1986). Topography of the afferent connectivity of area 17 in the macaque monkey: A double-labelling study. *Journal of Comparative Neurology* **253**, 374–402.

PESSOA, V.F., ABRAHÃO, J.C.H., PACHECO, R.A., PEREIRA, L.C.M., MAGALHÃES-CASTRO, B. & SARAIVA, P.E.S. (1992). Relative sizes of cortical visual areas in marmosets: Functional and phylogenetic implications. *Experimental Brain Research* **88**, 459–462.

PREUSS, T.M. & GOLDMAN-RAKIC, P.S. (1991). Architectonics of the parietal and temporal association cortex in the strepsirhine primate *Galago* compared to the anthropoid primate *Macaca*. *Journal of Comparative Neurology* **310**, 475–506.

PREVIC, F.H. (1990). Functional specialization in the upper and lower visual fields in man: Origins and implications. *Behavioral and Brain Sciences* **13**, 519–575.

ROCKLAND, K.S. & PANDYA, D.N. (1979). Laminar origins and terminations of cortical connections of the occipital lobe in the rhesus monkey. *Brain Research* **179**, 3–20.

ROSA, M.G.P., SOUSA, A.P.B. & GATTASS, R. (1988). Representation of the visual field in the second visual area in the *Cebus* monkey. *Journal of Comparative Neurology* **275**, 326–345.

ROSA, M.G.P., GATTASS, R., FIORANI, M., JR. & SOARES, J.G.M. (1992). Laminar, columnar, and topographic aspects of ocular dominance in the primary visual cortex of *Cebus* monkeys. *Experimental Brain Research* **88**, 249–264.

SANIDES, F. (1972). Representation in the cerebral cortex and its areal lamination patterns. In *The Structure and Function of the Nervous Tissue*, ed. BOURNE, G.H., pp. 329–453. New York: Academic Press.

SERENO, M.I. & ALLMAN, J.M. (1990). Cortical visual areas in mammals. In *Vision and Visual Dysfunction Vol. 4: The Neural Basis of Visual Function*, ed. LEVENTHAL, A.G., pp. 160–172. London: Macmillan.

SERENO, M.I., MCDONALD, C.T. & ALLMAN, J.M. (1987). Multiple visual areas between V2 and MT in the owl monkey. *Society for Neuroscience Abstracts* **13**, 625.

SHIPP, S. & ZEKI, S.M. (1985). Segregation of pathways leading from area V2 to areas V4 and V5 of macaque monkey visual cortex. *Nature* **315**, 322–324.

SOUSA, A.P.B., PIÑON, M.C.G.P., GATTASS, R. & ROSA, M.G.P. (1991). Topographic organization of cortical input to striate cortex in the *Cebus* monkey: A fluorescent tracer study. *Journal of Comparative Neurology* **308**, 665–682.

SPATZ, W.B. (1977). Topographically organized reciprocal connections between areas 17 and MT (visual area of the superior temporal sulcus) in the marmoset *Callithix jacchus*. *Experimental Brain Research* **27**, 559–572.

SPATZ, W.B. & TIGGES, J. (1972). Experimental-anatomical studies on the "middle temporal visual area" (MT) in primates. I. Efferent cortico-cortical connections in the marmoset *Callithrix jacchus*. *Journal of Comparative Neurology* **146**, 451–464.

SPATZ, W.B., TIGGES, J. & TIGGES, M. (1970). Subcortical projections, cortical associations, and some intrinsic interlaminar connections of the striate cortex in the squirrel monkey (*Saimiri*). *Journal of Comparative Neurology* **140**, 155–174.

STEELE, G.E., CUSICK, C.G. & WELLER, R.E. (1991). Cortical connections of the caudal subdivision of the dorsolateral area (V4) in monkeys. *Journal of Comparative Neurology* **306**, 495–520.

TIGGES, J., SPATZ, W.B. & TIGGES, M. (1973). Reciprocal point-to-point connections between parastriate and striate cortex in the squirrel monkey. *Journal of Comparative Neurology* **148**, 481–490.

TIGGES, J., TIGGES, M., ANSCHEL, S., CROSS, N.A., LETBETTER, W.D. & MCBRIDE, R.L. (1981). Areal and laminar distribution of neurons interconnecting the central visual cortical areas 17, 18, 19, and MT in squirrel monkey (*Saimiri*). *Journal of Comparative Neurology* **202**, 539–560.

TOOTELL, R.B.H., SILVERMAN, M.S., DE VALOIS, R.L. & JACOBS, G.H. (1983). Functional organization of the second visual area in primates. *Science* **220**, 737–739.

TUSA, R.J., PALMER, L.A. & ROSENQUIST, A.C. (1979). Retinotopic organization of areas 18 and 19 in the cat. *Journal of Comparative Neurology* **185**, 657-678.

UNGERLEIDER, L.G. & DESIMONE, R. (1986*a*). Projections to the superior temporal sulcus from the central and peripheral field representations of V1 and V2. *Journal of Comparative Neurology* **248**, 147-163.

UNGERLEIDER, L.G. & DESIMONE, R. (1986*b*). Cortical connections of visual area MT in the macaque. *Journal of Comparative Neurology* **248**, 190-222.

UNGERLEIDER, L.G., DESIMONE, R. & MORAN, J. (1986). Asymmetry of central and peripheral inputs from area V4 into the temporal and parietal lobes of the macaque. *Society for Neuroscience Abstracts* **12**, 1182.

UNGERLEIDER, L.G. & MISHKIN, M. (1979). The striate projection zone in the superior temporal sulcus of *Macaca mulatta*: Location and topographic organization. *Journal of Comparative Neurology* **188**, 347-366.

UNGERLEIDER, L.G. & MISHKIN, M. (1982). Two cortical visual systems. In *Analysis of Visual Behavior*, ed. INGLE, D.J., GOODALE, M.A. & MASNFIELD, R.J.W., pp. 549-586. Cambridge: MIT Press.

VAN ESSEN, D.C. & MAUNSELL, J.H.R. (1980). Two-dimensional maps of the cerebral cortex. *Journal of Comparative Neurology* **191**, 255-281.

VAN ESSEN, D.C., MAUNSELL, J.H.R. & BIXBY, J.L. (1981). The middle temporal visual area in the macaque: Myeloarchitecture, connections, functional properties, and topographic organization. *Journal of Comparative Neurology* **199**, 293-326.

VAN ESSEN, D.C., NEWSOME, W.T., MAUNSELL, J.H.R. & BIXBY, J.L. (1986). The projections from striate cortex (V1) to areas V2 and V3 in the macaque monkey: Asymmetries, areal boundaries, and patchy connections. *Journal of Comparative Neurology* **244**, 451-480.

VAN ESSEN, D.C. & ZEKI, S.M. (1978). The topographic organization of rhesus monkey prestriate cortex. *Journal of Physiology* (London) **277**, 193-226.

VON BONIN, G. & BAILEY, P. (1947). *The Neocortex of Macaca mulatta*. Urbana, Illinois: University of Illinois Press.

WALL, J.T., SYMONDS, L.L. & KAAS, J.H. (1982). Cortical and subcortical projections of the middle temporal area (MT) and adjacent cortex in galagos. *Journal of Comparative Neurology* **211**, 193-214.

WELLER, R.E. & KAAS, J.H. (1985). Cortical projections of the dorsolateral visual area in owl monkeys: The prestriate relay to inferior temporal cortex. *Journal of Comparative Neurology* **234**, 35-59.

WELLER, R.E., STEELE, G.E. & CUSICK, C.G. (1991). Cortical connections of dorsal cortex rostral to VII in squirrel monkeys. *Journal of Comparative Neurology* **306**, 521-537.

WELLER, R.E., WALL, J.T. & KAAS, J.H. (1984). Cortical connections of the middle temporal visual area (MT) and the superior temporal cortex in owl monkeys. *Journal of Comparative Neurology* **228**, 81-104.

WONG-RILEY, M. (1978). Reciprocal connections between striate and prestriate in squirrel monkey as demonstrated by combined peroxidase histochemistry and autoradiography. *Brain Research* **147**, 159-164.

ZEKI, S.M. (1971*a*). Convergent input from striate cortex (area 17) to the cortex of the superior temporal sulcus in the rhesus monkey. *Brain Research* **28**, 338-340

ZEKI, S.M. (1971*b*). Cortical projections from two prestriate areas in the monkey. *Brain Research* **34**, 19-35.

ZEKI, S.M. (1974). Functional organization of a visual area in the posterior bank of the superior temporal sulcus of the rhesus monkey. *Journal of Physiology* (London) **236**, 549-573.

ZEKI, S.M. (1978). The third visual complex of the rhesus monkey prestriate cortex. *Journal of Physiology* (London) **277**, 245-272.

ZEKI, S.M. (1980). A direct projection from area V1 and V3A of the rhesus monkey visual cortex. *Proceedings of the Royal Society B* (London) **207**, 499-506.